Angewandte Chemie International Edition

Angewandte International Edition Chemie

GDCh German Chemical Society

How to cite: *Angew. Chem. Int. Ed.* **2026**, e9566631
doi.org/10.1002/anie.9566631

REVIEW OPEN ACCESS

Rapidly Diversifying Hydrogen-Bonded Organic Frameworks With Permanent Porosity

Taito Hashimoto | Ichiro Hisaki

Division of Chemistry, Graduate School of Engineering Science, The University of Osaka, Toyonaka, Osaka, Japan

Correspondence: Ichiro Hisaki (i.hisaki.es@osaka-u.ac.jp)

Received: 30 April 2026 | **Revised:** 10 June 2026 | **Accepted:** 22 June 2026

Keywords: hydrogen bond | pi-conjugated molecule | porous molecular crystal

ABSTRACT

Throughout the long history of porous molecular crystals (PMCs), hydrogen-bonded organic frameworks (HOFs) have experienced a renaissance and have advanced significantly over the past two decades. HOFs can yield large single crystals with fewer defects due to their reversible bonding and dissociation processes, enabling precise analysis of the structure-property relationship. They are also attracting attention as candidates for sustainable materials. This article reviews the evolution of HOFs (primarily those with permanent porosity) over the past 15 years, based on the molecular structures of their constituent molecules (tectons). HOFs have been synthesized from a wide variety of tectons, ranging from simple substituted benzene derivatives to those with various π-conjugated polycyclic aromatic cores, as well as with rigid or flexible macrocyclic cores. Subsequently, we would like to focus on several distinctive aspects and concepts of HOFs. These include permanent porosity of rigid HOFs and flexible HOFs, which is crucial for porous materials; isostructural (isoreticular) HOFs, which can provide a series of continuous HOF libraries; and non-stoichiometrically mixed multicomponent HOFs, which aim to tune functions and create new ones by using multiple types of constituent molecules.

1 | Introduction: A Little Bit of History and Recent Trends

The 2025 Nobel Prize in Chemistry was awarded to Susumu Kitagawa, Richard Robson, and Omar M. Yaghi for their pioneering development of Metal-Organic Frameworks (MOFs) [1]. The construction of regular, infinitely extended frameworks with permanent porosity, composed of metal cations and organic ligands, is making waves beyond basic science and into industry as game-changing functional materials. The history of porous molecular crystals with internal voids dates back to the 1950s. Crystals of urea with one-dimensional (1D) channels [2] and crystals of Dianin's compound (4-*p*-hydroxyphenyl-2,3,4-triethylchroman) with hourglass-shaped cavities [3] are representative examples of early structures. Much of the research focused on these crystals from the perspective of inclusion crystals, which incorporate solvent molecules. In 1976, Barrer et al. reported the permanent porosity of Dianin's compound based on gas adsorption experiments on its crystals [4]. However, the complex interplay of multiple interactions, involving van der Waals forces that govern the formation of the structure, has made the systematic construction of porous crystals challenging. In 2011, Chen redefined porous molecular crystals formed via hydrogen bonding as hydrogen-bonded organic frameworks (HOFs) [5] and demonstrated selective sorption of C_2H_2 over C_2H_4 using Wuest's inclusion compound [6]. It was a renaissance of porous organic crystals. Since then, numerous HOFs have been constructed based on supramolecular synthons formed by functional groups such as diaminotriazine (DAT), carboxy, amino, and pyridyl groups. In recent years, the hydrogen bonds used in the construction of HOFs have expanded to include even weaker interactions, such as those between fluorine and hydrogen atoms, between a

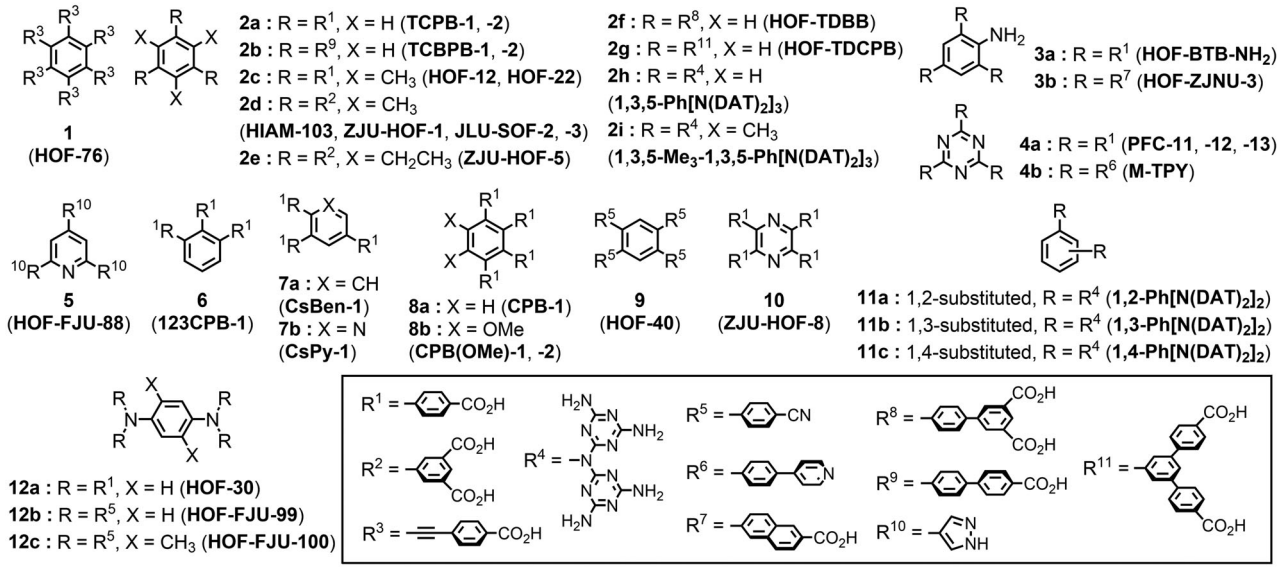

FIGURE 1 | Tectons based on benzene and analogous cores.

nitro group and an aromatic hydrogen atom, and between a cyano group and an aromatic hydrogen atom, enabling the creation of flexible HOFs capable of dynamic changes of pore shapes. So far, guest-responsive changes in fluorescence color and the separation of hydrocarbon isomers have been demonstrated for such flexible HOFs.

With the rise of HOF chemistry, many related review articles have been published, referring to HOF design [7–9], dynamic behaviors [10–12], selective gas adsorption and separation [13–15], fabrication of separation membranes [16, 17], catalytic function [18, 19], and composites with biomaterials [20, 21]. In this review, we provide an overview of the HOFs reported since our previous review [8], focusing on the rapidly diversifying structures of HOFs with permanent porosity. In the construction of HOFs, charge-assisted hydrogen bonding is a very powerful tool [22, 23]. However, these will not be discussed in this review due to space limitations. In the latter half of this review, we focus on permanent porosity and isostructurality (isoreticularity) of HOFs, which have been important aspects of porous materials. Moreover, the concept of non-stoichiometrically mixed multi-component HOFs will be introduced. Although this has been extensively reported in other types of framework materials, such as MOFs and COFs, there have been few reports on HOFs because they tend to settle into thermodynamically favorable single-component or stoichiometric cocrystalline HOFs. However, this is now being achieved through various structural innovations.

2 | Diversifying Skeletal Structures of Tectons

2.1 | Benzene Derivatives and Analogs

Substituted benzene derivatives and their analogs are the simplest entry of tectons for constructing HOFs (Figure 1). Hexatopic tecton **1** with carboxyphenylethynyl arms forms a three-dimensional (3D) H-bonded network via H-bonded dimerization of the carboxy groups, giving **HOF-76** that shows permanent porosity with Brunauer–Emmett–Teller surface area (SA_{BET}) of 1121 m^2g^{-1} and selective C_2H_4 uptake over C_2H_6 [24]. Two-dimensional (2D), ***hcb***-network-based, nonpenetrated, layered HOF **TCPB-1** is constructed by tritopic tecton **2a**, while **2b** with longer arms gives an 11-fold interpenetrated framework **TCBPB-1** composed of a nonplanar bowl-like 2D ***hcb***-network [25]. Tecton **2c** gives a honeycomb (***hcb***) network, which is polycatenated to give **HOF-12** with a degree of catenation (Doc) of (5/5) [26]. The tecton also gave **HOF-22** with a 2-fold interpenetrated structure, where two carboxylic groups form a H-bonded dimer, and the other forms a hydrogen bond with EtOH [27]. Tecton **2d** was investigated by three groups independently. The tecton yields three types of HOFs **JLU-SOF-2** [28], **JLU-SOF-3** [28], and **HIAM-103** [29] with different H-bonded motifs or interpenetration manners depending on crystallization conditions. Activation of **JLU-SOF-3** yields **ZJU-HOF-1**, which shows high C_2H_6 uptake capacity (88 $cm^3\,g^{-1}$ at 0.5 bar and 298 K) and excellent C_2H_6/C_2H_4 selectivity with the C_2H_4 productivity of 0.98 mmol g^{-1} [30]. Tecton **2e** yields highly porous HOF **ZJU-HOF-5** with a SA_{BET} of 3102 $m^2\,g^{-1}$, due to low interpenetration of the 3D networks [31]. Tecton **2f** forms a 3D 4-connected ***dia***-network, which is 2-fold interpenetrated to give **HOF-TDBB** [32]. Tecton **2g** forms a 3D 6-connected ***pcu***-network, which is 8-fold interpenetrated to yield **HOF-TDCPB** [33]. Tecton **2h** forms a highly open 3D ***noy***-network with a solvent-accessible volume of approximately 68% through 20 N—H···N bonds per molecule with five neighboring molecules [34]. Tecton **2i**, on the other hand, connects with six neighboring molecules through 12 N—H···N bonds to yield a highly open 3D ***cds***-network with an approximately 69% solvent-accessible volume [34]. Tecton **3a** forms a 2D hexagonal sheet, which develops a three-layered unit sheet through $\pi\cdots\pi$ stacking, followed by mutual polycatenation of the unit sheets to give **HOF-BTB-NH2** with Doc of (6/6), which shows high fluorescence quenching efficiency toward serotonin [35]. For analog **3b,** a four-layered unit sheet is mutually polycatenated to yield 3D networked **HOF-ZJNU-3** with Doc of (8/8) [36].

Nitrogen-containing analogs, on the other hand, show different assembly behaviors. Triazine-based tecton **4a** forms three types of entanglement isomers of HOFs, which are composed

of ***hcb***-networks with different undulation periods: HOFs **PFC-11**, **-12**, and-**13** exhibit Doc of 24, 18, and 36, respectively [37]. Tecton **4b** gives hollowed crystals of HOF **M-TPY** with micro- and microporosity [38]. The formation mechanism of the crystal is explained by highly anisotropic crystal growth due to the difference in energy among the highly oriented $\pi\cdots\pi$, C—H···N, and side-on interactions during diffusion-limited and supersaturated conditions. Pyridine-based tecton **5** yields 2D-layered HOF **HOF-FJU-88** composed of a hexagonal 2D network, which is formed through N—H···N bonds of pyrazole groups [39]. The HOF exhibits a notable selectivity for CO_2 over C_2H_2 with an IAST selectivity index of 1894.

C_{2v}-Symmetric tritopic tecton **6**, where the point group with the highest symmetry is presented without considering molecular conformation and the same applies below, gives a 6^3-connected 2D network, which is slip-stacked to give layered HOF **123CPB-1** [40]. C_s-Symmetric tetratopic tectons **7a** and **7b** yield ladder-shaped 1D network structures, which are slip-stacked and aligned in a coplanar manner to give HOFs, **CsBen-1** and **CsPy-1**, respectively [41]. Similar to **7**, C_{2v}-symmetric tetratopic tectons **8a** and **8b** yield ladder-shaped HOFs **CPB-1** and **CPB(OMe)-1**, respectively, in which the ladder motifs stack in different manners, forming discrete voids in the former and 1D inclusion channels in the latter [42]. Tetratopic tecton **9** forms a 3D 6-connected ***pcu***-network through two types of 12 intermolecular C—H···N≡C bonds. The network is 2-fold interpenetrated to yield **HOF-40** [43]. The framework has a gate-opening nature and exhibits superior separation performance for Xe/Kr mixtures. Tecton **10** with four carboxyphenyl groups directing alternately up and down gives **ZJU-HOF-8** with 4-fold interpenetrated ***dia*** networks [44]. The HOF has flexible, robust pores and shows significant uptake of C_3H_8 and *n*-C_4H_{10} compared with smaller hydrocarbons C_2H_6 and CH_4 under ambient conditions. Similar to **2i**, tectons **11** gave complex frameworks with various topologies, such as ***cds*** and ***vco***, due to flexible conformations and versatile H-bonding patterns of the DAT groups. Among them, **11b** formed a framework with a guest-accessible volume of 74% [34]. Tecton **12a** is connected by two kinds of hydrogen bonds, conventional carboxy dimers and alcohol-bridged carboxy dimers, to yield **HOF-30** that possesses 10-fold interpenetrated 3D ***dia***-networks. The activated HOF afforded the sole usual carboxy dimers and showed the selective adsorption of propyne over propylene [45]. Analogs **12b** and **12c** with cyano groups form similar wavy, layered HOFs, **HOF-FJU-99** and **HOF-FJU-100**, respectively, which are constructed through multiple intermolecular interactions such as C—H···π, C—H···N≡C, and $\pi\cdots\pi$ interactions [46]. **HOF-FJU-99** is nonporous, whereas **HOF-FJU-100** exhibits microporosity, because the methyl groups of **12c** serve as the grafting units to form the pore structures between the layers. **HOF-FJU-100** showed unparalleled separation efficiency and ultrahigh selectivity for C_2H_2/CO_2 mixtures.

Applying a highly symmetric benzene as a platform enables the formation of well-defined H-bonded networks. Many tectons were synthesized based on combinations of the benzene cores with different substitution positions and substituent numbers, H-bonding functional groups, and linker structures, resulting in the development of versatile HOFs. Particularly, carboxylic acid-based tectons provide systematic construction of HOFs in terms of molecular geometries and network topologies due to their well-predictable supramolecular synthons, while the incorporation of pyridine and cyano groups with weak H-bonding capability enables the construction of stimuli-responsive flexible HOFs.

2.2 | Oligophenylene and Related Skeletons

Tectons with biphenyl, terpenyl, and related skeletons are the second simplest entry of tectons (Figure 2). Tecton **13** forms a 3D ***dia***-network via H-bonded dimerization of the carboxy groups. The network is 4-fold interpenetrated to give HOF **BPTCA-1** with 1D hexagonal-shaped pores [47]. The activated HOF **BPTCA-2** shows high absorption selectivity toward naphthalene over anthracene. Tecton **14** yields 7-fold interpenetrated, robust HOF **HOF-15** with SA_{BET} of 1964 m^2g^{-1} [48]. Tecton **15** gives a 6-fold interpenetrated, robust HOF **ZJU-HOF-10** that exhibits high separation ability for C_2H_6 from the mixture of C_2H_6 and C_2H_4 [49]. Tecton **16** yields 4-fold interpenetrated robust HOF **HOF-20**, showing highly efficient and selective turn-on fluorescent sensing of aniline in water [50].

Tecton **17a** yields 2D-layered HOF **TPTCA-1**, in which the 2D network constructed via H-bonded dimerization of the carboxy groups is slip-stacked. Activated HOF **TPTCA-2** exhibits selective absorption of anthracene over naphthalene [47]. Tecton **17b** gives a 2D-layered HOF composed of 2D-lamellar networks via H-bonding between DAT groups [51]. Tectons **18a** and **18b** yield 2D-layered HOFs, **BTIA-1** [52] and **BTTA-1** [53], respectively, via the dimerization of the carboxy groups and dipole-dipole interaction of benzo[*c*][1,2,5]thiadiazole (BT) cores. These HOFs exhibit photoconductivity due to the 1D-stacked structure of BT moieties [53]. Tecton **18c** forms a 2D-layered HOF isostructural with that constructed from **17b** [51]. Tecton **19** yields 2D-layered HOF **ABTPA-1** through the dimerization of the carboxy groups and $\pi\cdots\pi$ stacking between the anthracene cores. The stacking manner changes from parallel (**ABTPA-1**) to herringbone (**ABTPA-2**) upon guest removal [54]. Tecton **20** yields a 2D-layered HOF **NTTA-1**, in which the naphthalene moieties are accumulated in parallel-stacking manners [55]. Tectons **21a**, **21b**, **21c**, **21d** yield 2D-layered HOFs, **ZJU-HOF-59, ZJU-HOF-60**, **ZJU-HOF-61** and **ZJU-HOF-62** respectively. Their staking structures are different depending on the core moieties [56, 57]. Tecton **22** forms a 2D-layered HOF **NDITA-1** that possesses π-stacked columnar domains and pore channels surrounded by NDI planes, resulting in significant changes in absorption and emission spectra as well as electron conductivity upon exchange of aromatic guest solvents [58].

When core structures of tectons are changed from benzene to biphenyl, the resulting HOFs tend to have a 3D-networked and interpenetrated structure with thermal stability and permanent porosity, due to the twisted conformation of the tectons. On the other hand, the tectons with terphenyl moieties generally yield 2D-networked structures, which is because the central aryl ring is twisted and the terminal aryl rings adopt a coplanar conformation. Furthermore, skeletal elongation can yield layered HOFs with a larger void. However, no HOFs composed of tectones with longer cores than quaterphenylene have been reported, presumably due to the low solubility of the tectones and/or the structural instability of the resulting HOFs.

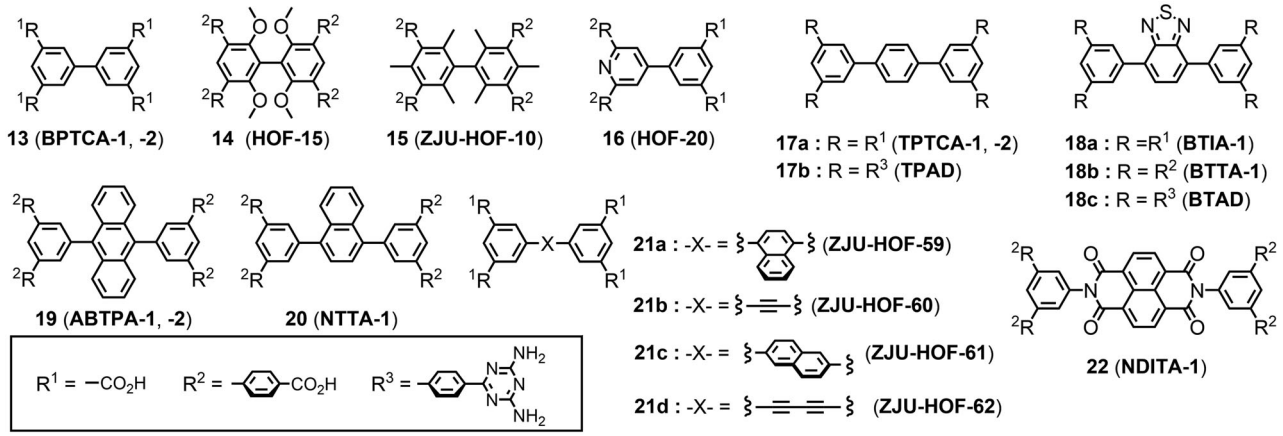

FIGURE 2 | Biphenyl- and terphenyl-based and related tectons.

2.3 | PAH and Related Cores

Tectons with various rigid polycyclic aromatic hydrocarbon (PAH) skeletons provide a wide range of HOFs from structural and functional points of view (Figure 3). Pyrene is one of the most frequently used PAH cores for tectons. 1,3,6,8-Substituted pyrene-based HOFs tend to yield robust 2D-layered HOFs stabilized by strong $\pi\cdots\pi$ interactions between pyrene cores [59]. Tectons **23a–d** give layered HOFs composed of ***sql***-topological 2D networks constructed via the dimerization of carboxy groups [60]. Tecton **24a**, possessing BT arms, yields ***sql*** 2D-layered HOF **PFC-111** that promotes the generation rate of single oxygen (quantum yield = 0.98) [61]. Tecton **24b** possesses carboxy-naphthalene forms ***sql***-networked, 2D-layered HOF **HOF-14** with a high SA_{BET} of 2572 m^2g^{-1} [62]. Tecton **24c** possessing *m*-carboxyphenyl arms also gives isoreticular HOF **FDU-HOF-3**, showing reversible structural transformation between the crystalline and amorphous phases by exposing to NH_3 gas [63]. Tecton **24d** yields 2D-layered HOF **FDU-HOF-5** via H-bonding of DAT groups. The HOF displays selective fluorescence quenching toward diethyl chlorophosphate [64]. Tecton **24e** forms an infinite H-bonded helical chain through N—H···N bonds between pyrazole groups, and these chains interconnected the molecules into 3D HOF **HOF-FJU-168** that features two distinct channels shaped like a parallelogram and rhombus [65]. The HOF exhibited Xe/Kr separation performance with an excellent balance of adsorption capacity and selectivity. Tecton **25**, a configurational isomer of **24a**, yields ***sql***-networked, 2D-layered HOF **CP-Py-1**, whose interlayer interaction is not a $\pi\cdots\pi$ interaction between pyrene cores, but C—H$\cdots\pi$ interactions between the hydrogen atoms of peripheral phenylene rings and the pyrene cores [66]. Hexahydrogenated analog **26** gives HOF **CP-Hp-1** with a nearly identical structure to **CP-Py-1** [67]. These HOFs exhibited framework shrinkages upon guest removal [66, 68]. Tecton **27a** yields a ***sql***-networked, 2D-layered HOF with good crystallinity, while **27b** gives a low-crystalline HOF [69]. These HOFs can produce photocatalytic H_2O_2 under visible light irradiation. NDI-based tectons yield HOFs with photochromic and electrochromic properties. Tecton **28a** forms 1D networks through single hydrogen bonds of carboxy groups, and the network assembles via H-bonding with $[NH_2(CH_3)_2]^+$ ions to give electrochromic HOF **ECUT-HOF-30** [70]. Tecton **28b** yields ***sql***-networked, 2D-layered HOF **HOF-DAT** through N—H···O bonds between DAT groups and NDI cores, and complementary N—H···N bonds of DAT groups [71]. The HOF showed excellent electrochemical performance for Na^+ ion storage. Tecton **29a**, possessing a hexaazatrinaphthylene (HATN) moiety, yields layered HOF **CPHATN-1** composed of H-bonded ***hxl***-network sheets [72]. The HOF shows reversible color changes from yellow to reddish-brown in response to acid vapors, due to the protonation of the HATN cores. Tecton **29b**, an isomer of **29a**, yields HOF **CPBTQ-1** that also responds to acid vapors [73].

X-Shaped tetracarboxylic acid derivatives **30a**, **30b**, **30c**, **31a**, and **31b** give layered HOFs, **CP-NT-1** [74], **CP-QX-1** [74], **CP-PP-1** [74, 75], **X-PyQ-1** [76], and **Br-PQ-1** [77], respectively, composed of H-bonded, ***sql***-topological network sheets. These HOFs undergo drastic structural transformation involving cleavage and rearrangement of H-bonded networks upon guest removal. Tectons **32a** and **32b** with similar molecular structures yield HOFs **TAAQ-1** and **AQ-1** with different network structures: the former has the ***sql***-network, whereas the latter has a triangle network motif [78]. However, both HOFs undergo the structural transformation with the hydrogen bond reformation. TTF is an attractive redox-active molecular platform for constructing HOFs with electronic functionality. Tecton **33a** yields ***sql***-networked, 2D-layered HOF **PFC-77** that exhibits structural changes involving H-bonding rearrangement and layer slipping upon guest exchanges [79]. Its redox property changed upon the structural transformation. Tecton **33b** gives rigid, ***sql***-networked, 2D-layered HOF **HOF-110,** and iodine-incorporated HOF **HOF-110@I_2** afforded pressed pellets conductivity values of up to 6.0×10^{-7} S·cm^{-1} [80]. Tecton **33c** forms C≡N···H—C bonds to give flexible HOF **HOF-FJU-106** that exhibits a temperature-dependent gate opening phenomenon [81]. This behavior enabled enhanced gas adsorption and separation performance for binary C_3H_6/C_3H_8 mixtures.

Tetra- and hexacarboxyphenyl-substituted tectons possessing a twisted PAH core, such as dibenzo[*g,p*]chrysene (DBC) and hexaazatriphenylene (HAT), form 3D networks with ***dia***- or ***pcu***-topology through the dimerization of carboxy groups, and the networks give 3D frameworks via interpenetration of the networks and shape-fitted docking of the twisted cores. DBC-based tectons **34a**, **34b**, **34c**, and **34d** yield 6-fold, 8-fold, 4-fold, and 4-fold interpenetrated HOFs **CPDBC-1**, **C2N6DBC-1**, **C1N4DBC-1** and **C1N5DBC-1**, respectively [82, 83]. **CPDBC-1** retains the original

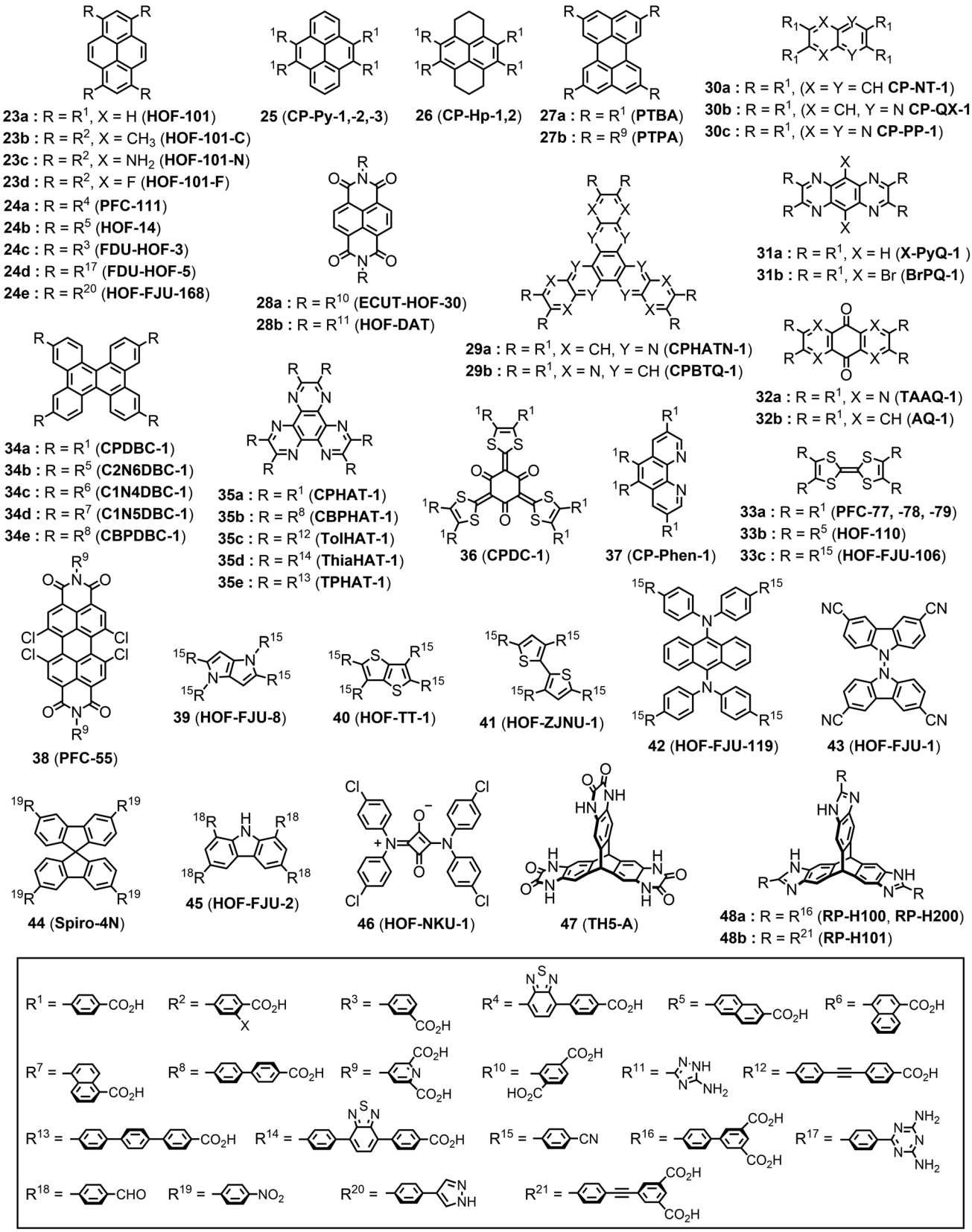

FIGURE 3 | PAH-based and related tectons.

structure after activation, whereas **C2N6DBC-1**, **C1N4DBC-1**, and **C1N5DBC-1** show activation-induced structural transformation behaviors depending on the naphthyl substituents upon guest removal [83]. HAT-based tecton **35a**, **35b, 35c**, **35d** form 4-fold, 6-fold, 8-fold, and 8-fold, interpenetrated isostructural 3D HOFs **CPHAT-1**, **CBPHAT-1**, **TolHAT-1**, **ThiaHAT-1**, respectively, although tecton **35e** did not give a HOF [84–86].

A D_{3h}-symmetric tecton **36**, possessing a tri(dithiolylidene) cyclohexanetrione unit, forms an anomalistic 3D helical H-bonded network via the dimerization of carboxy groups, which originated from a slightly larger bite angle between adjacent carboxy phenyl groups in the molecule, to yield 3D HOF **CPDC-1** [87]. Tecton **37** yields solvent-included porous framework **CP-Phen-1**, in which three of four carboxy groups form H-bonded dimers to form the ladder-shaped framework, while the remaining one does not due to geometrical mismatch and alternately interacts with guest molecules through weak H-bonding [88]. Tecton **38**, possessing a twist perylenediimide (PDI) core, forms wave-like 2D networks through two types of H-bonding of carboxy groups. The networks are interpenetrated and stacked via $\pi\cdots\pi$ interactions between PDI cores to give HOF **PFC-55** [89].

PAH tectons bearing cyano groups tend to form 2D-networked structures through multiple types of C≡N···H—C bonds between cyano groups and aromatic hydrogen atoms. These networks are assembled to yield flexible HOFs with small pores. Tecton **39** yields **HOF-FJU-8** possessing 1D channels with a 4.6 × 4.2 Å aperture. The activated HOF exhibited high C_2H_2/CO_2 and Xe/Kr separation performances [90, 91]. Tecton **40** gives 2D-layered HOF **HOF-TT-1** possessing 1D channels with a 9.0 × 10.9 Å aperture that shows selective absorption of toluene over methylcyclohexane, accompanied by a change in fluorescence color [92]. Tecton **41** yields robust 2D-layered HOF **HOF-ZJNU-1** via donor-acceptor $\pi\cdots\pi$ interactions between the thiophen and benzene rings. The HOF possesses 1D channels with a 3.7 × 4.2 Å aperture and exhibits selective absorption of acetylene and carbon dioxide over methane [93]. Tecton **42** forms a 2D-layered HOF **HOF-FJU-119** possessing 1D channels with a 4.9 × 9.7 Å aperture. The activated HOF shows framework expansion to restore its original pore structure upon guest absorption and exhibits selective absorption of benzene over cyclohexane [94]. Tecton **43** forms a H-bonded 3D network through complementary C≡N···H—C bonds. The network is 3-fold interpenetrated to yield **HOF-FJU-1** possessing 1D channels with a 3.4 × 5.3 Å aperture [95, 96]. The activated HOF exhibited tunable flexible-robust framework properties depending on temperature, resulting in selective adsorption of C_2H_4 over C_2H_6 [96].

Tecton **44** forms HOF **Spiro-4N** through C—H···O and C—H···π weak bonds. The HOF displays selective fluorescence quenching for aniline and diphenylamine among various aromatic solvents [97]. Tecton **45** forms **HOF-FJU-2** through multiple weak interactions. The HOF possesses 1D channels with a 4.8 × 6.1 Å aperture surrounded by a carbazole N—H site, allowing separation of acetone from its mixture with another solvent like methanol [98]. Tecton **46** yields flexible HOF **HOF-NKU-1** through multiple weak hydrogen bonds, such as C—H···O = C and C—H···C bonds. The HOF exhibits high SO_2/CO_2 separation performance through temperature-dependent gate-opening [99].

Tecton **47** yields one of the most porous HOF **TH5-A**, composed of a 3D network formed through H-bonding of quinoxalinedione groups [100]. Tecton **48a** forms a hexagonal unit through single O—H···O bonding of carboxy groups, which further interpenetrates with adjacent units through hydrogen bonds between imidazole moieties and carboxy groups to yield 7-fold catenated HOF **RP-H100** [101]. Alternatively, the same tecton utilizes N—H···O and O—H···N bonding between these two functional groups to give the hexagonal unit; two of these hexagonal units then interpenetrate and connect via O—H···O bonding of carboxy groups to yield another HOF, **RP-H200**, possessing hexagonal mesopores with a width of 36 Å [102]. Tecton **48b**, an extended analogue of **48a**, yields HOF **RP-H101** that is isostructural to **RP-H100**, displaying highly balanced volumetric and gravimetric capacities for hydrogen storage [101].

As described above, PAHs and hetero-PAHs can provide HOFs with optoelectronic functionality in addition to thermodynamic stability through $\pi\cdots\pi$ stacking between PAH cores. Particularly, large π-conjugated or twisted π-conjugated skeletons can form a robust $\pi\cdots\pi$ stacked domain, which serves as the basis for the construction of isoreticular HOFs as discussed later. It is also significant from a photoelectronic point of view, and active research is underway to apply this to photocatalytic HOFs. Particularly, introducing heteroatoms into PAHs results in even richer electronic properties, such as redox behavior and charge transport capabilities. The interaction between the nonbonding electron pairs of heteroatoms and cations enables the modulation of electronic states, opening up possibilities for applications such as chemical sensors.

2.4 | Cyclic and Caged Cores

Cyclic and caged tectons can further diversify structures and properties of HOFs (Figure 4). Porphyrin is a useful molecular platform for porous frameworks because it can exhibit diverse properties simply by changing the central metal in the porphyrin core without altering its molecular geometry. Tecton **49a** forms a ***sql***-networked 2D sheet through the dimerization of carboxy groups. The sheet is assembled in an ABAB stacking manner to yield layered HOF **PFC-71** [103]. Crystallization of **49b** from a DMF/methanol mixed solution leads to the formation of 3D-networked HOF **UPC-H4a** with 1D hexagonal channels through multiple types of H-bonding between DAT groups [104]. In contrast, crystallization from a DMF/acetone mixed solution produces 2D-layered HOF **FDU-HOF-2** with rhombic 1D channels. The HOF is composed of a ***sql***-topological 2D network sheet formed through head-to-head interaction of DAT groups and further head-to-waist interactions of DAT groups [105]. Tecton **49c** is connected via C—H···N bonds between nitrogen atoms of the tetrazole and hydrogen atoms of the porphyrin moiety to give 2D networks, which are stacked through N—H···N and C—H···N interactions to give 2D-layered HOF **JZS-1** [106]. Tecton **49d** forms 2D networks through C—H···N≡C bonds, and these networks are slipped stacked to give 2D-layered HOF **HOF-29**, which shows exclusive recognition of *p*-xylene over its isomers of *o*-xylene and *m*-xylene triggered by the HOF's structural transformation with the sliding of the layers [107]. Metalloporphyrin-based tectons **50a–d** yield 2D-layered HOFs, as in the case of non-metalloporphyrinic tecton **49a**, although the

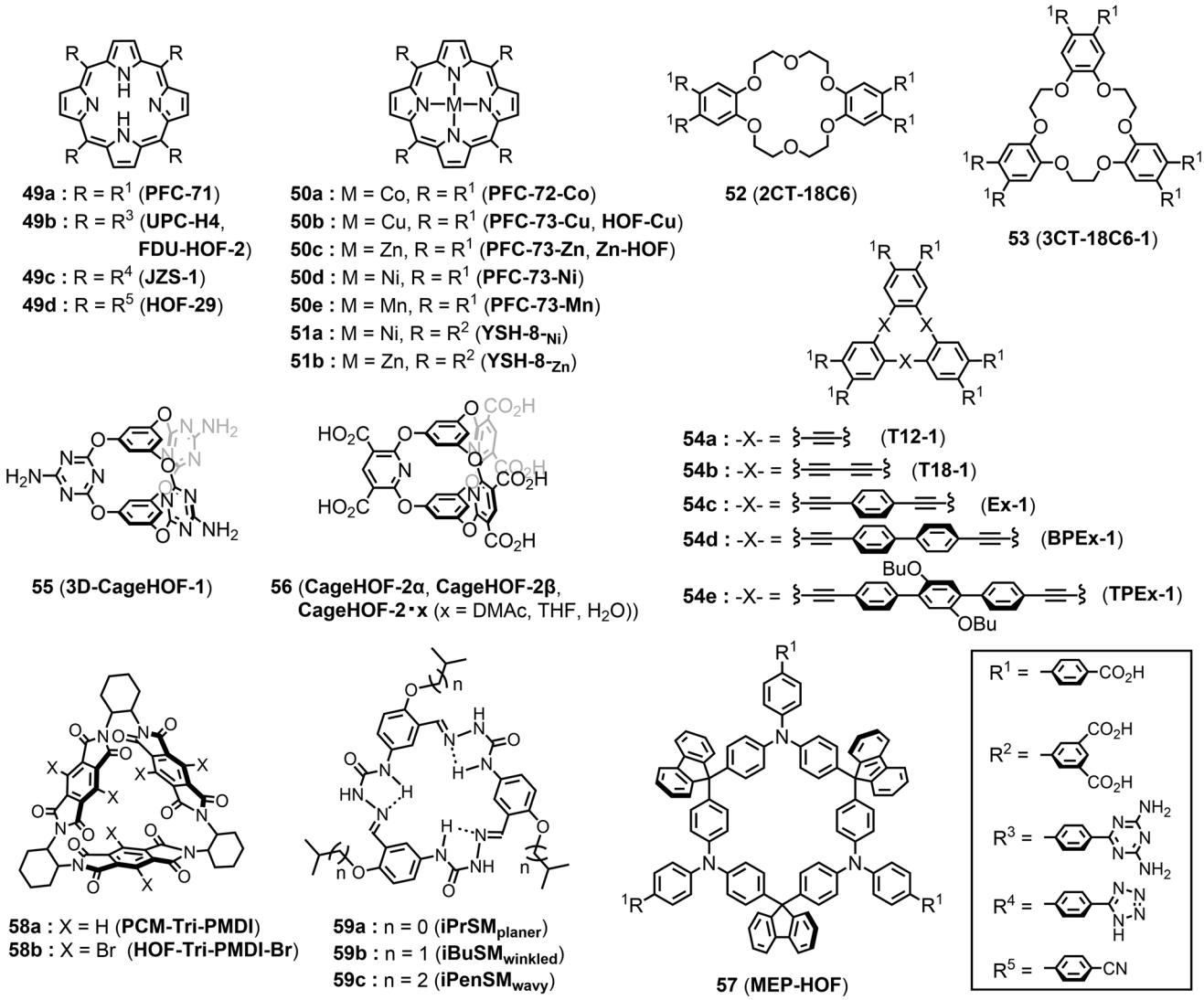

FIGURE 4 | Cyclic and caged molecules-based tectons.

stacking structure of 2D networks varies depending on the metals [103]. Tecton **50e** also yields 2D-layered HOF **PFC-73-Mn**, in which water molecules interact with the Mn ions and bridge the porphyrin layers [108]. Tectons **51a** and **51b**, possessing tetrakis-3,5-dicarboxyphenyl groups, give 4-fold and 2-fold interwoven 3D networked HOFs, **YSH-8$_{Ni}$** and **YSH-8$_{Zn}$**, respectively [109]. The HOFs are further stabilized by $\pi\cdots\pi$ interaction among porphyrin cores.

18-Crown-6-ether (18C6)-based tetracarboxylic acid **52** is connected through water-bridged H-bonding of the carboxy groups to give HOF **2CT-18C6-III**, which possesses unique 1D water molecule alignments and exhibits proton conductivity [110]. 18C6-Based hexacarboxylic acid **53** yields layered HOF **3CT-18C6-I** composed of a H-bonded hexagonal sheet [111]. The HOF features 1D channels with bottlenecks composed of the 18C6 rings, resulting in proton conductivity. D_{3h}-Symmetric macrocyclic molecules **54a, 54b, 54c, 54d**, and **54e** form robust H-bonded hexagonal network sheets with three kinds of voids. The sheets are stacked without interpenetration to yield 2D-layered HOFs **T12-1**, **T18-1**, **Ex-1**, **BPEx-1**, and **TPEx-1**, respectively [112]. Notably, **BPEx-1** possesses the largest hexagonal 1D pores with a width of 24 Å due to the large overlap of the hexagonal frameworks [113], and **TPEx-1** features the largest hexagonal void with a size of 30 × 34 Å [114]. Cage-shaped tecton **55** is connected through N—H···N bonds between the NH_2 group and triazine ring to give low-density (0.54 g cm^{-3}) mesoporous HOF **3D-Cage-HOF-1** [115]. Tecton **56** yields various HOFs with different crystal structures, **CageHOF-2*α***, **CageHOF-2*β***, **CageHOF-2**·DMA, **CageHOF**·2-THF, and **CageHOF-2**·H_2O, depending on the crystallization conditions, which are attributed to "hinge-like" rotational motions of the molecules [116].

D_{3h}-Symmetric fluorenylidene-aza[1$_6$]cyclophane derivative **57** forms wavelike 2D ***hcb***-networks through the dimerization of carboxy groups due to its flattened cone-like geometry, and the networks are interpenetrated to yield **MEP-HOF** that shows significant fluorescence quenching for nitrobenzene [117]. Trimeric pyromellitic diimide derivatives **58a** and **58b** yield 3D networked HOFs, **PMC-Tri-PMDI** and **HOF-Tri-PMDI-Br**, respectively [118]. The former is constructed by H-bonding between the hydrogen atoms of phenylene rings and the O═C groups of

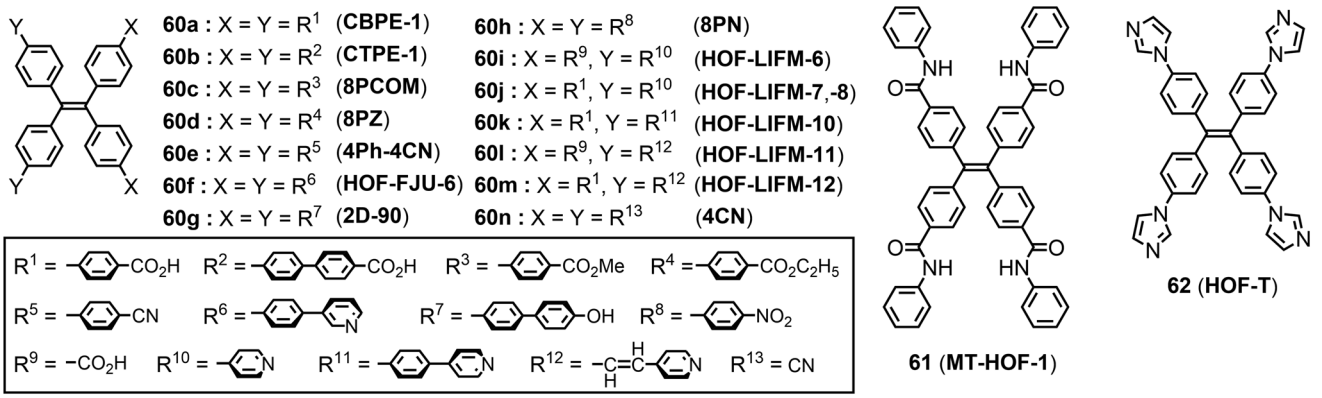

FIGURE 5 | TPE-based tectons.

the imide moieties, whereas the latter is formed via unusual H-bonding between the C(sp_3)-H of the cyclohexane rings and the O═C groups. C_3-Symmetric tectons **59a, 59b,** and **59c** are assembled through 3-fold self-complementary N—H···O═C bonds to give planar, wrinkled, and square-octagonal wavy 2D networks, respectively, which are stacked to give 2D-layered HOFs **iPrSM$_{planar}$**, **iBuSM$_{wrinkled}$**, and **iPenSM$_{wavy}$** [119]. The distorted frameworks exhibited record-high acetone vapor uptake (up to 617 cm^3/g STP at 298 K) with high acetone/methanol selectivity (up to 7.2:1).

Since macrocyclic molecules inherently possess internal cavities, it is possible to construct HOFs with multiple pores of different properties. On the other hand, relatively lower yields of cyclization reactions required for the synthesis of cyclic molecules often hinder the development of macrocycle-based HOFs.

2.5 | Tetraphenylethene

Tetraphenylethene (TPE), which exhibits aggregation-induced emission, can provide HOFs that possess rich luminescent properties (Figure 5). Tecton **60a** forms a 2D ***sql***-network sheet via the dimerization of carboxy groups, and the sheets are assembled via tri-axially interpenetration to yield mechanically-responsive fluorescent HOF **CBPE-1** [120]. Tecton **60b**, in contrast to **60a**, yields non-interpenetrated 2D-layered HOF **CTPE-1**, possessing large rhombic voids with a 33.6 × 55.2 Å aperture [121]. HOF **8PCOM** composed of **60c** changes its crystal structure responding to different solvent vapors, and DCB-solvated HOF **8PCOM-DCB** exhibits strong emission intensity owing to the alignment of the dipole moments of the four ketone groups [122]. HOF **8PZ**, composed of **60d**, possesses outstanding adaptive guest accommodation abilities for 3-alkylthiophenes (denoted **SCX**, where X (X = 1–10) represents the number of carbon atoms in its alkyl chain) and shows reversible fluorescence changes upon the release of **SCX** [123]. Tecton **60e** yields two types of HOFs with different topologies, cage-type HOF and channel-type HOF, depending on the guest solvent used for crystallization. These HOFs can reversibly switch their structures upon soaking in the corresponding guest solvents, accompanied by changes in fluorescence colors [124]. Tecton **60f** is connected by C—H···π interactions, to yield **HOF-FJU-6** that shows reversible framework shrinkage and expansion via desorption and adsorption of guest molecules, leading to the reversible fluorescence change between blue and green [125]. Tecton **60g** yields two solvated HOFs, ethyl acetate-solvated HOF (**2D-90**) and methanol-solvated HOF (**2D-82**), which exhibit reversible structural transformation between them upon exposure to the solvent vapors [126]. HOF **8PN**, composed of **60h**, shows versatile reversible transformations accompanied by changes in its luminescence property upon guest exchange [127]. Tectons **60i–n**, featuring substituents comprising pyridine and carboxylic acid groups conducive to hydrogen bond formation, yield **HOF-LIFM-6**, **HOF-LIFM-7**, **HOF-LIFM-8**, **HOF-LIFM-10**, **HOF-LIFM-11**, and **HOF-LIFM-12**, respectively [128]. This series of HOFs exhibits exceptional cell imaging capabilities due to the excellent one- and two-photon excited luminescence properties. HOF **4CN**, composed of **60n**, exhibits versatile reversible structural transformations and fluorescence changes under the stimulation of solvent vapor and temperature [129]. Tecton **61** forms a 1D column by linking up and down through N—H···O bonds between the amide groups, and the four columns are interlocked in pairs to yield **MT-HOF-1** [130]. The HOF showed clear separation trends for C_2H_6/C_2H_4. Tecton **62** is connected through C—H···N bonding between the nitrogen atoms of the imidazole groups and the hydrogen atoms of the benzene ring/imidazole of adjacent molecules to give **HOF-T** that possesses the ability to capture UO_2^{2+} selectively [131].

As described above, TPE-based HOFs alter their dynamic emission colors by structural transformations with the changes in molecular conformation and aggregation states. TPE-based tectons with weak H-bonding supramolecular synthons particularly tend to yield flexible HOFs, whose photophysical properties are sensitively modulated by guest absorption/desorption or guest exchange.

2.6 | Amine

Triarylamine is a representative platform of nonplanar tritopic tectons (Figure 6). Tecton **63** yields two different HOFs, **HOF-11** and **HOF-16,** that are obtained by crystallization from a THF/hexane mixed solution and a methanol solution, respectively. In **HOF-11**, all the carboxyl groups form H-bonded dimers to give 3D networks, followed by forming a multiply-interpenetrated framework with small 1D channels [132]. In **HOF-16**, two carboxyl groups form a H-bonded dimer, and

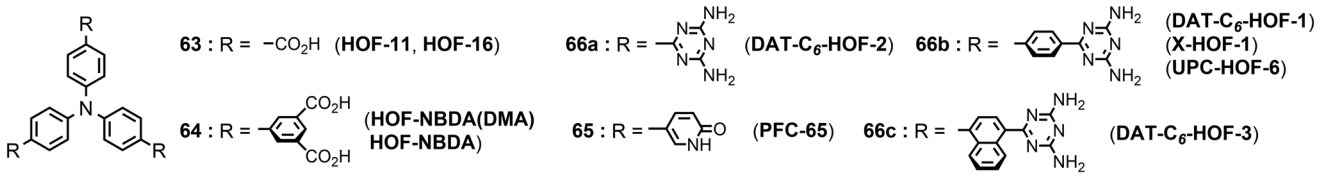

FIGURE 6 | Triarylamine-based tectons.

the other forms hydrogen bonds with two methanol molecules to yield 1D-helical chains, and these chains are assembled to form 1D channels with exposed carboxylic acid groups [133]. Tecton **64** yields ***hcb***-like 2D-layered HOF **HOF-NBDA(DMA)**, in which four carboxy groups form classical neutral dimers and the other two form rarely seen COOH···$^{-}$OOC single hydrogen bonds. Dimethylamine (DMA) cation molecules are trapped in the carboxylate of the 2D networks by N—H···O bonds. **HOF-NBDA(DMA)** transforms into **HOF-NBDA** upon heating, accompanied by the removal of DMA molecules and the reorganization of hydrogen bond dimers [134]. **HOF-NBDA** exhibited much higher absorption selectivity for C_2H_6 over C_2H_4 than **HOF-NBDA(DMA)**, owing to its nonpolar void surface. Tecton **65** forms N—H···O bonds of pyridone groups to give a hexagonal 2D network, and the four monolayer networks interpenetrated to construct 3D HOF **PFC-65** with a ***hcb***-topological network [135]. The HOF modified on a glassy carbon electrode showed high sensitivity, stability, and precise identification of dopamine molecules in various environments. Tectons **66a**, **66b**, and **66c** yield a series of isoreticular HOFs **DAT-C_6-HOF-1,2,3**, with (6,3)-net ***hcb***-topology by integrated monomer synthesis-framework assembly methodology. **DAT-C_6-HOF-1** displayed highly selective fluorescence recognition of perfluorooctanoic acid over other homologous molecules [136]. Crystallization of **66b** from DMSO/methanol and DMF/water mixed solutions gives the polymorph HOFs **X-HOF-1** [137] and **UPC-HOF-6** [138], respectively, featuring nearly the same 2D-layered structure composed of H-bonded networks with rhombic voids and abnormal hexagon voids. **X-HOF-1** possessed pressure-responsive H_2/N_2 separation performance, and **UPC-HOF-6** exhibited fluorescence change from green to orange-yellow upon exposure to acetic acid vapors.

3 | Permanent Porosity

We investigated the Brunauer–Emmett–Teller surface area (SA_{BET}) of 126 HOFs reported from 2020 to 2025. To facilitate discussion, we classified the HOFs into rigid HOFs that retain their original structures and flexible HOFs that undergo structural transformation after activation. The values of SA_{BET} are plotted against their publication year (Figure 7). Note that HOFs whose SA_{BET} has not been reported are excluded from these plots. The data of SA_{BET} are summarized in Table S1. The HOFs exhibiting exceptionally high SA_{BET} are mainly those possessing a triptycene skeleton, highlighted as follows. HOF **RP-H101** [101], composed of **48b**, shows the highest SA_{BET} of 3526 $m^2\ g^{-1}$ among HOFs reported to date. HOF **TH5-A** [100], composed of **47**, shows SA_{BET} of 3284 $m^2\ g^{-1}$, which is the third highest ever reported after **T2-γ** [139]. HOF **RP-H200** [102], composed of **48a**, exhibits the largest pore size reported to date (3.6 nm) with a SA_{BET} of 2313 $m^2\ g^{-1}$. Other HOFs with high SA_{BET} are **ZJU-HOF-5** [31], composed of 1,3,5-tris(3,5-dicarboxyphenyl)-2,4,6-triethylbenzene **2e**, with SA_{BET} of 3102 $m^2\ g^{-1}$, and **HOF-14** [62], composed of tetrakiscarboxynaphthyl pyrene derivative **24b**, with SA_{BET} of 2573 $m^2\ g^{-1}$.

The SA_{BET} values are compared among the HOFs constructed by the molecules with common moieties (Table 1). The SA_{BET} of 1,3,8,11-substituted pyrene-based HOFs, which have rigid 2D-layered structures, tends to increase as their pore size becomes larger. However, this is not always the case; for example, **FDU-HOF-5** [64] has larger pores than **PFC-1** [59] and **HOF-14** [62], while its SA_{BET} is smaller, suggesting that framework rigidity after activation also plays a role in SA_{BET}. The HAT-based HOFs with rigid structures exhibit large SA_{BET} as the arm lengths increased (**CPHAT-1**< **CBPHAT-1**< **ThiaHAT-1**), whereas fragile HOF **TolHAT-1** showed small SA_{BET} [86]. Similarly, in DBC-based HOFs, structural rigidity significantly influences the SA_{BET}; robust HOFs such as **CPDBC-1** and **C1N5DBC-1** exhibit larger SA_{BET}, whereas fragile or flexible HOFs such as **C1N4DBC-1** and **C2N6DBC-1** show smaller SA_{BET} [82, 83]. In the case of porphyrin-based HOFs, metalloporphyrin HOFs tend to show larger SA_{BET} compared to the corresponding metal-free HOF **PFC-71** [103], due to enhanced framework rigidity, while the type of metal has little effect on SA_{BET}. The HOFs composed of 5,5′-substituted bis-isophthalate derivatives, which have 2D-layered structures, show larger SA_{BET} as the core lengths increased (**ZJU-HOF-59**< **ZJU-HOF-60**< **ZJU-HOF-61**< **ZJU-HOF-62**) [56]. Based on the above discussion, not only pore size but also framework rigidity plays an important role in achieving large SA_{BET}.

Flexible HOFs have rapidly increased in number since around 2022. They tend to exhibit smaller SA_{BET} than rigid HOFs because they exhibit a reduction in pore size and, sometimes, decreasing of crystallinity upon solvent removal (i.e., activation). On the other hand, by utilizing their small pore sizes and/or flexible pore transformations (e.g., pore expansions and gate-opening behaviors), many flexible HOFs have achieved selective adsorption of target molecules and efficient separation of mixed gases (Table 2). For example, in **ZJU-HOF-8a**, its flexible pore pockets selectively open to accommodate larger alkanes like *n*-C_4H_{10} and C_3H_8 due to their stronger binding affinities. This adsorbate-induced framework expansion allows for significantly higher uptake of these molecules, resulting in high adsorption selectivity over C_2H_6 and CH_4, which cannot trigger the gate-opening behavior [44]. **HOF-NKU-1** exhibits a shape-memory effect accompanied by a guest-adaptive pore expansion that is specifically triggered by strong intermolecular interactions with SO_2 molecules. Because CO_2 interacts too weakly to induce this structural transformation, the material achieves highly selective SO_2 capture through the dense packing of SO_2 dimers within the expanded cavities [99].

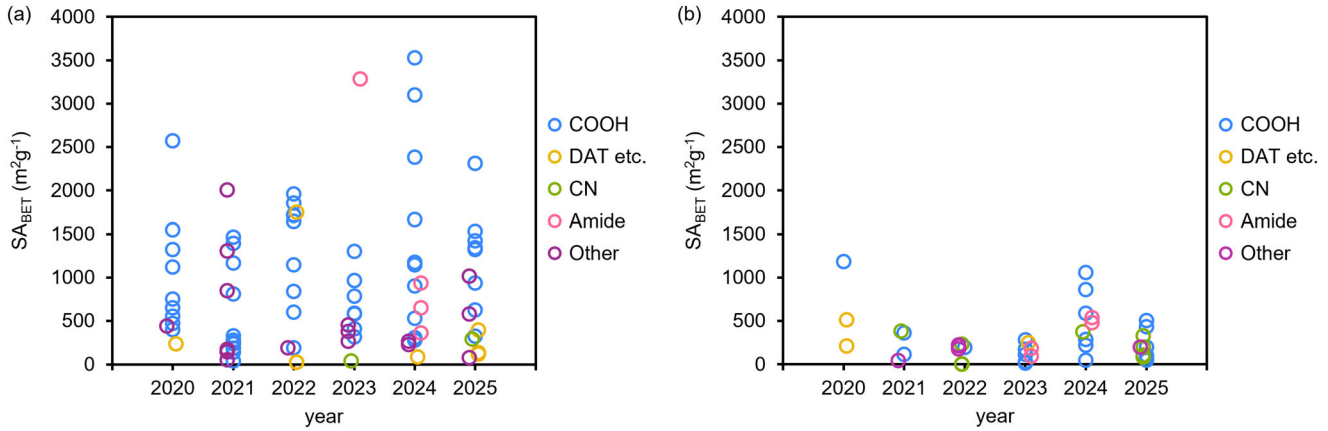

FIGURE 7 | BET surface areas of (a) robust HOF and (b) flexible HOF reported in the period from 2020 to 2025.

TABLE 1 | Comparison of SA_{BET} values of HOFs composed of tectons with the same skeleton.

Skeleton	HOF	SA_{BET} (m^2g^{-1})	Stability	Tecton	Refs.
1,3,6,8-Substituted pyrene	**PFC-1**	2122	robust	**23a**	[59]
	HOF-101HCF	1148	robust	**23a, b, d**[a]	[60]
	PFC-111	1177	robust	**24a**	[61]
	HOF-14	2573	robust	**24b**	[62]
	FDU-HOF-3	310	robust	**24c**	[63]
	FDU-HOF-5	396	robust	**24d**	[64]
	HOF-FJU-168	1016	robust	**24e**	[65]
Hexaazatriphenylene (HAT)	**CPHAT-1**	649	robust	**35a**	[84]
	CBPHAT-1	1288	robust	**35b**	[85]
	TolHAT-1	440	fragile	**35c**	[86]
	ThiaHAT-1	1394	robust	**35d**	[86]
Dibenzo[*g*,*p*]chrysene (DBC)	**CPDBC-1**	1548	robust	**34a**	[82]
	C2N6DBC-1	113	fragile	**34b**	[83]
	C1N4DBC-1	281	flexible	**34c**	[83]
	C1N5DBC-1	1300	robust	**34d**	[83]
Porphyrin	**PFC-71**	600	robust	**49a**	[103]
	PFC-72-Co	1646	robust	**50a**	[103]
	PFC-73-Cu	1714	robust	**50b**	[103]
	PFC-73-Zn	1856	robust	**50c**	[103]
	PFC-73-Ni	1720	robust	**50d**	[103]
	PFC-73-Mn	786	robust	**50e**	[108]
	JZS-1	222	flexible	**49c**	[106]
	YSH-8Ni	280	robust	**51a**	[109]
	YSH-8Zn	1665	robust	**51b**	[109]
5,5′-Substituted bis-isophthalate	**ZJU-HOF-59**	938	robust	**21a**	[56]
	ZJU-HOF-60	1057	robust	**21b**	[56]
	ZJU-HOF-61	1424	robust	**21c**	[56]
	ZJU-HOF-62	1534	robust	**21d**	[56]

[a]**HOF-101HCF** is a mixed-HOF composed of tectons **23a**, **23b**, and **23d**.

TABLE 2 | Flexible HOFs exhibiting pore expansion and gate-opening upon gas adsorption and their gas selectivity.

HOF	SA_{BET} (m^2g^{-1})	Tecton	Gas selectively	Ref
ZJU-HOF-8	863	**10**	C_3H_8, n-C_4H_{10} > CH_4, C_2H_6	[44]
ZJU-HOF-60	1057	**21b**	C_2H_6 > C_2H_4	[57]
HOF-FJU-8	375	**39**	C_2H_2 > CO_2, Xe > Kr	[90, 91]
HOF-FJU-100	328	**12c**	C_2H_2 > CO_2	[46]
HOF-FJU-119	106	**42**	C_6H_6 > C_6H_{12}	[94]
HOF-FJU-106	198	**33c**	C_3H_6 > C_3H_8	[81]
HOF-FJU-1	385	**43**	C_3H_6 > C_3H_8, C_2H_4 > C_2H_6	[95, 96]
HOF-40	234	**9**	Xe > Kr	[43]
HOF-NKU-1	200	**46**	SO_2 > CO_2	[99]

Next, we overview the permanent porosity of HOFs from the perspective of their H-bonded supramolecular synthons. Carboxylic acid-based HOFs tend to exhibit larger SA_{BET} than HOFs using other synthons, because self-complementary hydrogen bonds of the carboxy groups are highly directional and relatively stable (ca. 65 kJ mol^{-1}), allowing facile formation of stable HOFs with large voids. In particular, 2D-layered HOFs and 3D-HOFs stabilized by strong $\pi\cdots\pi$ interactions and shape-fitted π-conjugated cores often possess large channels, resulting in a high SA_{BET} value. Recently, carboxylic acid-based flexible HOFs have attracted considerable attention, which show the rearrangement [45, 74–79], shrinkage/expansion [66], and sliding [44, 140] of H-bonded networks upon guest absorption and desorption. Such flexible HOFs enable selective gas absorptions and guest-responsive emissions. Most of the DAT-based HOFs reported in recent years showed small SA_{BET}, because these HOFs were constructed through head-to-waist interactions of DAT groups, resulting in a small pore size. Cyanide-based HOFs tend to possess flexible pores due to weak C≡N···H—C bonds between a cyano group and a hydrogen atom of peripheral phenylene groups. Their flexible structures enable selective gas absorption and separation of mixed gases via pore expansion and gate opening mechanisms. While amide-based HOFs have been extensively studied primarily using triptycene-based mesoporous frameworks [139, 141], recent efforts have led to the construction of HOFs from amide derivatives with diverse core moieties, exhibiting a wide range of porosities. Over the past five years, HOFs using novel hydrogen bonding synthons, such as pyridine [38, 142], aldehyde [143], pyrazole [65, 144, 145], tetrazole [106], ketone [122], and chloro groups [99], have been reported. Most of them have relatively small pores and small SA_{BET}, and several systems have been demonstrated to show selective gas absorption properties [65, 98, 99, 144, 145].

4 | Updated Concepts of HOFs

4.1 | Isostructural (Isoreticular) HOFs

Isostructural porous frameworks, whose molecular arrangements and network topology are identical but with different pore sizes and/or chemical and physical properties, provide a systematic library of functional porous materials [146, 147]. Therefore, constructing such frameworks is considered a touchstone for reticular chemistry [148]. In the fields of MOFs and COFs, pore expansion can be readily achieved by elongating the length of ligand molecules or spacer moieties [149, 150]. In contrast, in the case of HOFs, it remains difficult to obtain isostructural frameworks even when using tectons with similar structures, due to the weakness of hydrogen bonds and the diversity in molecular packing modes. For example, tectons **54**, D_{3h}-symmetric π-conjugated planar building blocks possessing three *o*-bis(4-carboxyphenyl)benzene moieties, form the same ***hxl***-topological sheets; however, their stacking manners are different due to the lack of specific interlayer interactions (Figure 8) [112]. Similarly, tetraphenylethene-based tetracarboxylic acids **60a** and **60b** form common 2D ***sql***-networks but give different packing structures: the former has a polycatenated structure, whereas the latter forms a slipped-stacked, layered structure [120, 121].

On the other hand, utilizing shape-fitted docking of the molecules is a useful strategy to produce isostructural frameworks. HAT-base hexacarboxylic acids **35a–d** give nearly isostructural HOFs due to the shape-fitted docking of the HAT cores, and the size of the triangle pore can be expanded up to 20.4 × 19.2 Å (Figure 9a) [84–86]. DBC-base tetracarboxylic acids **34a–c** that possess 1,4-, 1,5-, and 2,6-substituted carboxynaphthyl groups also yield isostructural HOFs with different pore geometries due to the docking of the DBC cores (Figure 9b). They show different structural stabilities against activation [82, 83]. Most porphyrin-based tetracarboxylic acids yield ***sql***-networked, 2D-layered HOFs, in which stacking manners of the 2D networks can be either identical or different depending on the metal encapsulated within the porphyrin ring [103]. 1,3,6,8-Substituted pyrene-based tetracarboxylic acids **23a**, **23c**, and **24b** yield isostructural 2D-layered HOFs through strong $\pi\cdots\pi$ stacking of the pyrene core, which enables the modification of pore size and pore environment by changing the arm moieties of the tectons (Figure 9c) [59–63]. Tetracarboxylic acids **30a–c** with naphthalene, quinoxaline, and pyrazinopyrazine cores, respectively, yield isostructural 2D-layered HOFs, where ***sql***-networked sheets were slip-stacked in a closely similar manner through C—H···π interactions (Figure 9d), while these HOFs transformed into different structures upon the guest removal [74]. Terphenyl analogs **18b**, **19**, and **20** with π-conjugated moieties yield nearly

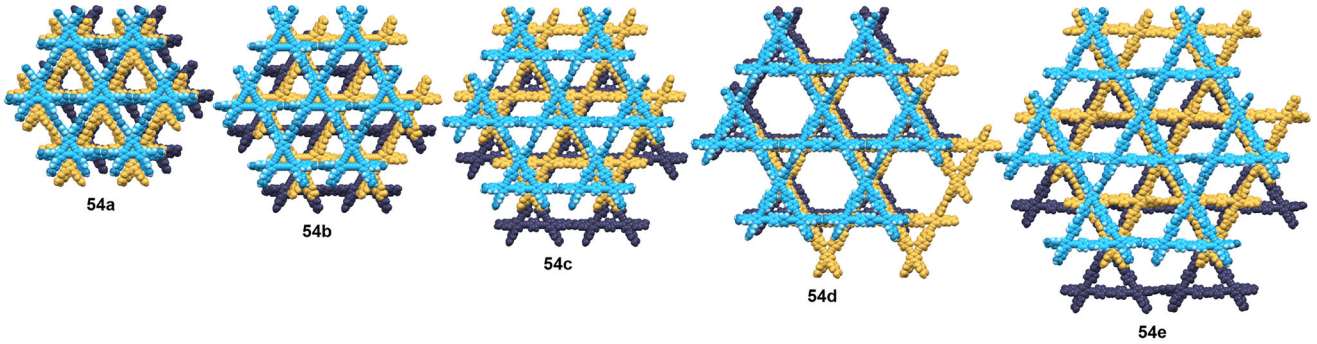

FIGURE 8 | Selected crystal structures of **T12-1** (**54a**), **T18-1** (**54b**), **Ex-1** (**54c**), **BPEx-1** (**54d**), and **TPEx-1** (**54e**). The tectons form the same ***hxl***-topological sheet, while the sheets stack in different ways depending on the cores. The butoxy side chains of molecule **54e** are omitted.

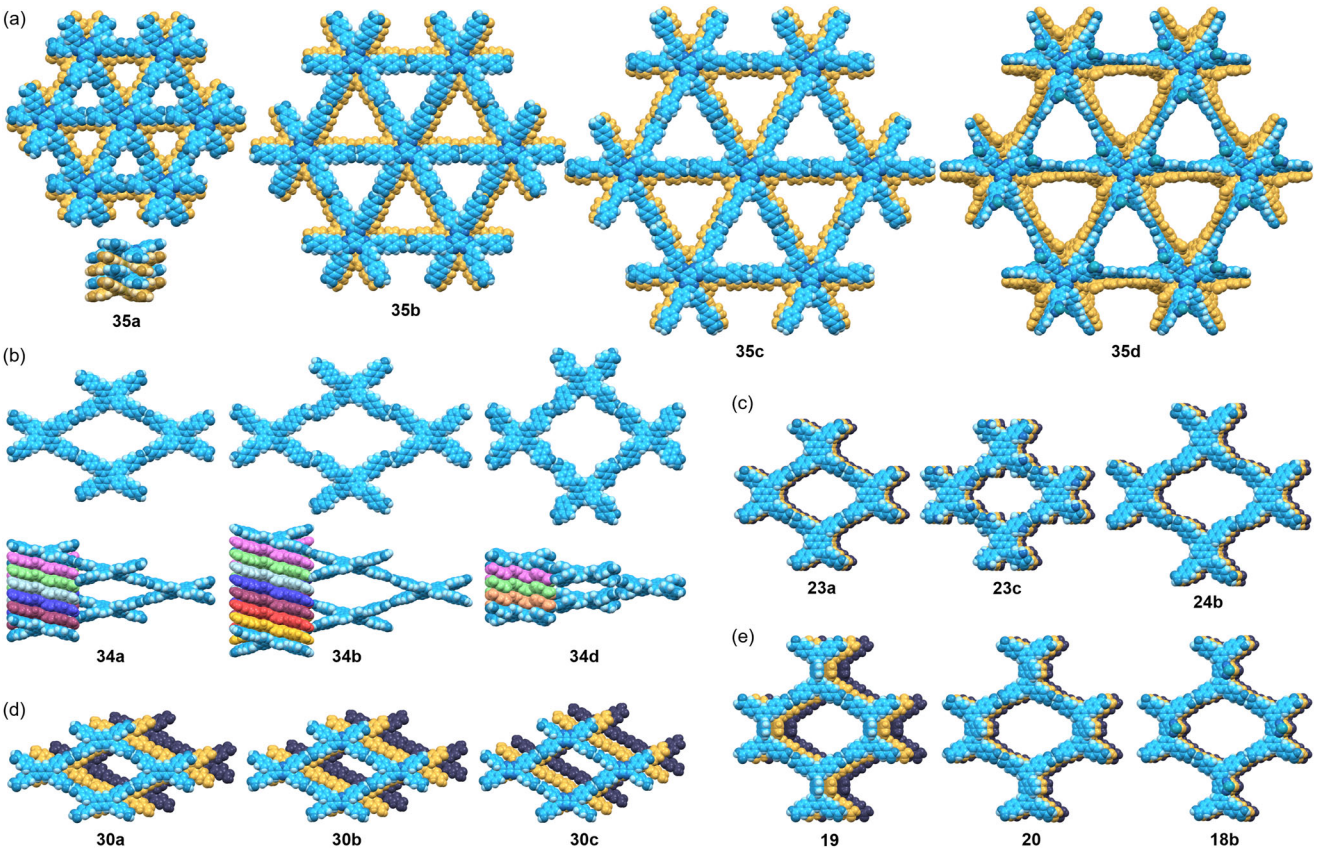

FIGURE 9 | Recently reported isostructural HOFs. (a) HAT-based HOFs **CPHAT-1** (**35a**), **CBPHAT-1** (**35b**), **TolHAT-1** (**35c**) and **ThiaHAT-1** (**35d**). (b) DBC-based HOFs **CPDBC-1** (**34a**), **C2N6DBC-1** (**34b**) and **C1N5DBC-1** (**34d**). (c) Pyrene-based HOFs **PFC-1** (**23a**), **HOF-101N** (**23c**), and **HOF-14** (**24b**). (d) HOFs with naphthalene and its analogue cores **CP-NT-1** (**30a**), **CP-QX-1** (**30b**), **CP-PP-1** (**30c**). (e) Terphenyl analogs-based HOFs **ABTPA-1** (**19**), **NTTA-1** (**20**), **BTTA-1** (**18b**).

isostructural 2D-layered HOFs, where the 2D networks were stacked through $\pi\cdots\pi$ interactions between the core moieties (Figure 9e) [53–55, 58].

Isostructural HOFs using supramolecular synthons other than carboxylic acid dimers have also been reported. Tetrahedral pyrazole derivatives with different cores yield isostructural HOFs, in which the molecules are connected through N—H···N bonding tetramers to give 4-fold interpenetrated diamond networks [145]. Tetra-imine oligomers form isostructural HOFs with 1D quasi-square pores, formed through C—H$\cdots\pi$ interactions and further stabilized via multiple hydrogen bonds [143].

4.2 | Mixed HOFs

Multicomponent mixed frameworks, in which two or more kinds of tectons are combined in various ratios, have attracted attention due to their ability to fine-tune material properties and generate new functions via compositional variation, and have been widely

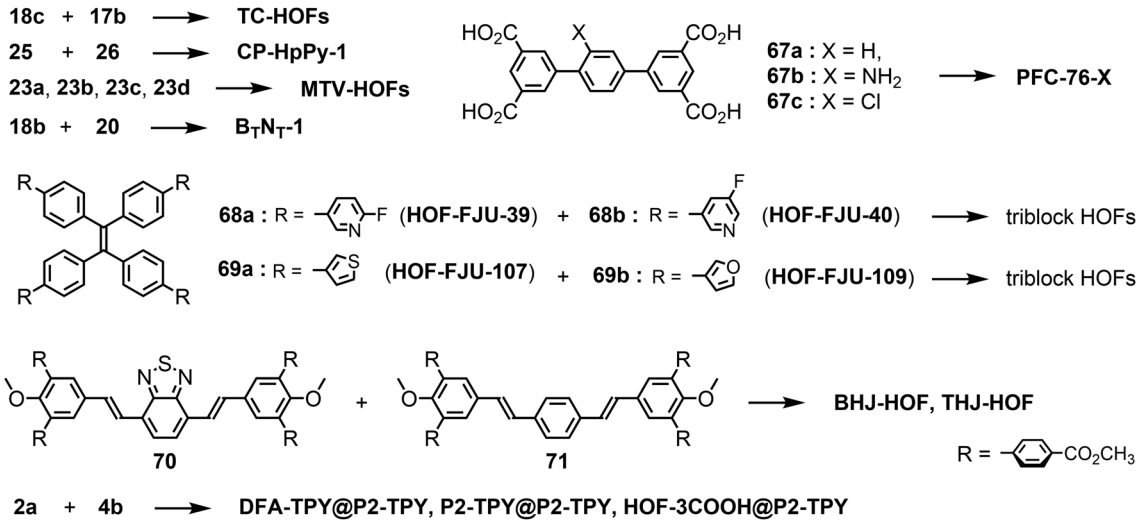

FIGURE 10 | A combination of tectons to prepare mixed HOFs.

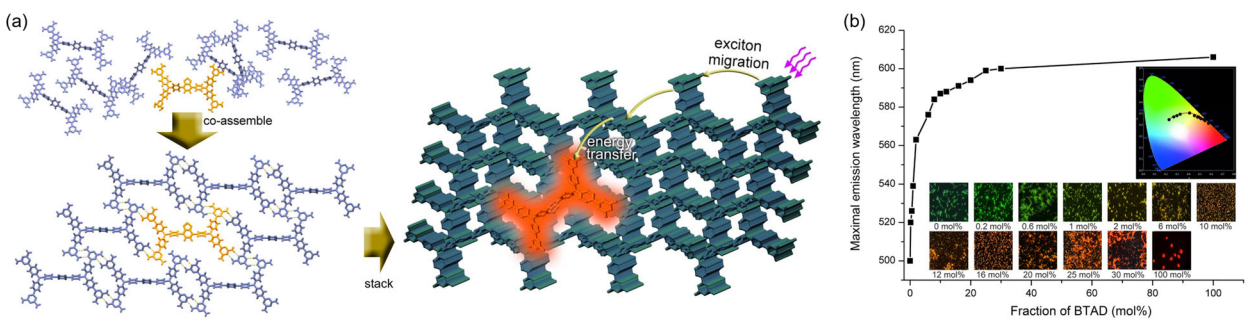

FIGURE 11 | (a) Schematic representation of the co-crystallization of **17c** and **18c** and energy transfer in **TC-HOF** with a low content of benzothiadiazole (BTAD) derivative **18c**. (b) Fluorescence images, CIE dots, and plot of emission maxima vs the fraction of **18c** for **TC-HOF** with various component ratios. Reproduced with permission from ref [51]. Copyright 2022, American Chemical Society.

studied in MOFs and COFs [151, 152]. Their strong coordination or covalent bonds facilitate the construction of mixed systems, leading to numerous reported examples. In contrast, HOFs tend to form thermodynamically stable single-component frameworks due to their relatively weak, reversible hydrogen bonds, making the construction of mixed HOFs challenging. This challenge, however, has recently been addressed by using tectons that can form isostructural HOFs as components of mixed HOFs (Figure 10) [153]. In particular, carboxylic acid-based mixed HOFs often exhibit high crystallinity, allowing detailed structural analysis and revealing correlations among composition, structure, and properties, thereby offering promising potential for further development.

As a pioneering work, Xue and coworkers reported **TC-HOFs** composed of **17b** and **18c** with DAT moieties [51]. The two molecules homogeneously distribute within the HOF, and the fluorescence color of bulk crystals of the HOF can be tuned by the component ratio due to the energy transfer from donor **17b** to acceptor **18c** (Figure 11). In this system, however, the precise structural analysis using single crystals was not reported, presumably due to the low crystallinity or size limitation of crystals. Our group demonstrated, for the first time, that pyrene- and hexahydropyrene-based tectons **25** and **26**, respectively, give single crystals of mixed HOFs **CP-HpPy-1** [67]. Single-crystal X-ray diffraction analysis and microscopic Raman spectroscopy revealed that the two kinds of tectons are contained in a single crystal with a similar composition ratio to the mixing ratio of the initial solution, while they are distributed heterogeneously and/or gradationally rather than homogeneously throughout the single crystal. (Figure 12). Since **CP-HpPy-1** was reported, various mixed HOFs and their property modulations by compositional variation of tectons have been demonstrated. They are mainly composed of carboxylic acids. 1,3,6,8-Substituted tetrakis(carboxyphenyl)pyrene derivatives bearing various functional groups (—H, —CH_3, —NH_2, and —F) on phenylene arms (**23a**, **23b**, **23c**, and **23d**, respectively) yield multicomponent mixed HOFs **MTV-HOF** with rigid structures and permanent porosities [60]. **MTV-HOF** exhibits tunable hydrophobicity depending on the component ratio in the frameworks and superior selective sorption properties for mustard gas simulant, 2-chloroethyl ethyl sulfide (CEES), from moisture (Figure 13). [1,1′:4′,1″-Terphenyl]-3,3″,5,5″-tetracarboxylic acids **67a**, **67b**, and **67c**, possessing functional groups (—H, —NH_2, and —Cl, respectively) on the central benzene, yield mixed HOFs **PFC-76-X** with tunable water adsorption performance by component ratios,

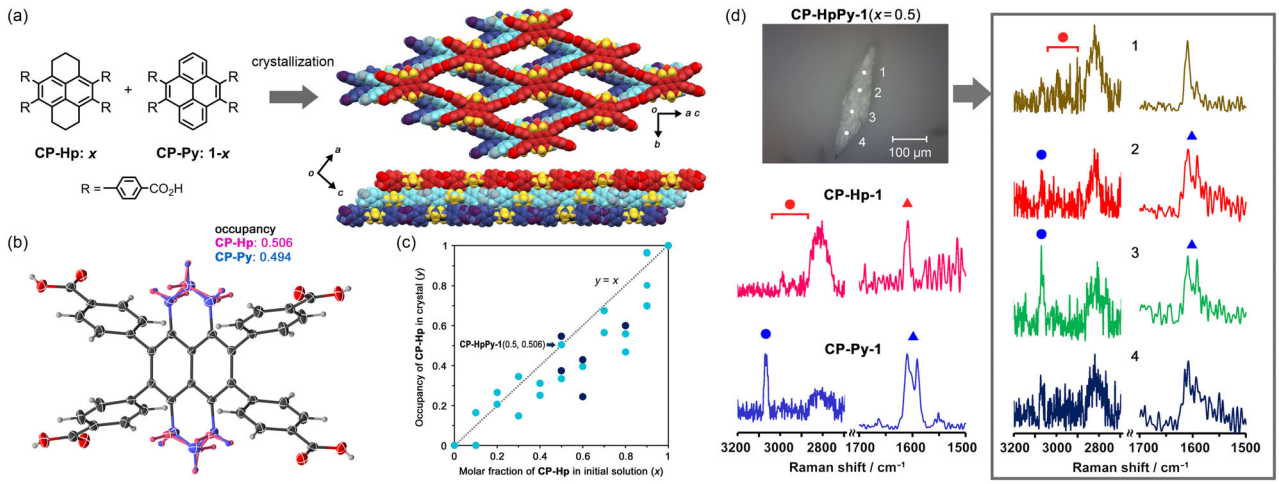

FIGURE 12 | Formation of mixed HOF **CP-HpPy-1** composed of tectons **25** and **26**. (a) Crystal structure of **CP-HpPy-1**, where yellow-colored parts indicate disordered propylene moieties of hexahydropyrene. (b) Anisotropic displacement ellipsoid plot with 50% probability for **CP-HpPy-1**(0.5, 0.506), in which the carbon atoms at the 1,2,3- and 6,7,8-positions are disordered in two structures corresponding to **CP-Hp** and **CP-Py**, with occupancies of 0.506 and 0.494, respectively. (c) Composition in single-crystals of **CP-HpPy-1**(x, y), where x and y denote the molar fraction or occupancy of **CP-Hp** in the initial solution and the resultant single crystal, respectively. For a certain x, the plots in different colors (i.e., cyan and dark blue) indicate that single crystals were selected from different batches. (d) microscopic Raman spectra of single-component HOF crystals of **CP-Hp-1** and **CP-Py-1** and mixed HOF **CP-HpPy-1**(x = 0.5), where spectra 1, 2, 3, and 4 were recorded at different positions numbered on the photographs of the single crystal shown at the top. Reproduced with permission from ref [67]. Copyright 2022 Wiley-VCH GmbH.

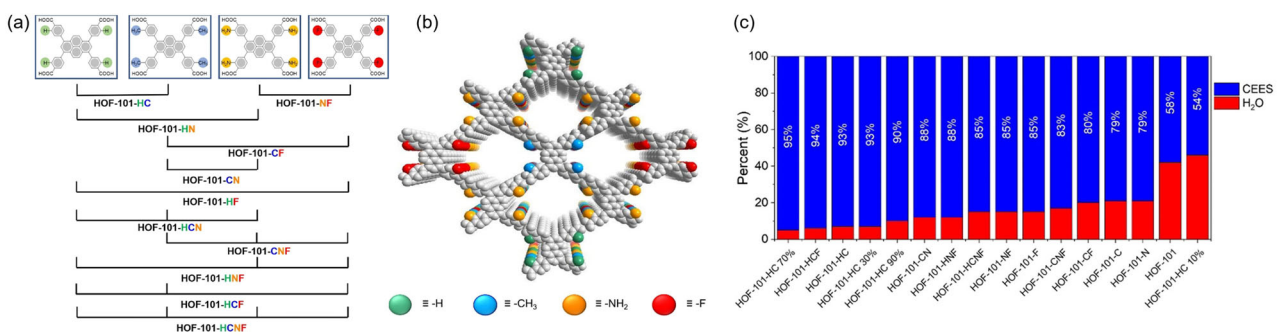

FIGURE 13 | Formation of multi-component HOF **MTV-HOF** based on **23a**, **23b**, **23c**, and/or **23d**. (a) Four **H_4TBAPy−R** (R = H, CH_3, NH_2, and F) tectons and **MTV-HOF-101** are synthesized with each other. (b) Schematic diagram of the structure of **MTV-HOF-101**. (c) Comparison of the water and CEES adsorption of **MTV-HOF-101** at 0.8 kPa. **HOF-101-C**, **HOF-101-N** and **HOF-101-F** means **HOF-101-R** (R = CH_3, NH_2 and F). Reproduced with permission from ref [60]. Copyright 2023 Wiley-VCH GmbH.

and **PFC-76-NH2–67%** with an optimized balance of pore size and adsorption sites achieves the highest water uptake within a narrow humidity range [154]. Terphenyl-based tetracarboxylic acids **18b** and **20**, possessing naphthalene and benzothiadiazole cores, yield fluorescent mixed HOF **B_TN_T-1** (Figure 14) [55]. Depending on the composition and distribution of the tectons, single crystals of **B_TN_T-1** exhibit a wide range of fluorescent colors, ranging from single colors such as blue, white, green, and yellow to dual emission colors such as blue-green and green-yellow.

Not only static property modulation but also dynamic property modulation has been achieved in mixed HOFs. **CP-HpPy-1** undergoes structural transformation from the open framework into the shrunk framework (**CP-HpPy-2**) by spontaneous release of the solvent molecules included in the pores. Interestingly, the transformation behaviors strongly depend on the composition ratio (Figure 15) [68]. The transformation speed changed not proportionally but nonlinearly with the composition ratio. The maximum speed of the transformation is observed when the composition ratio of tectons **25** and **26** is 1:1.

Mixed HOFs with heterogeneous structures, such as block-type or core–shell-type architectures, have also been reported, although only in a few cases. Block-type HOF systems that exhibit multimodal luminescent responses to external stimuli have been demonstrated for application in high-security anti-counterfeiting and information coding (Figure 16). Tetraphenylethene derivatives **68a** and **68b** produce the triblock single crystals of HOF heterostructure by a H-bond-assisted epitaxial growth method. The adopted HOFs, **HOF-FJU-39** and **HOF-FJU-40**,

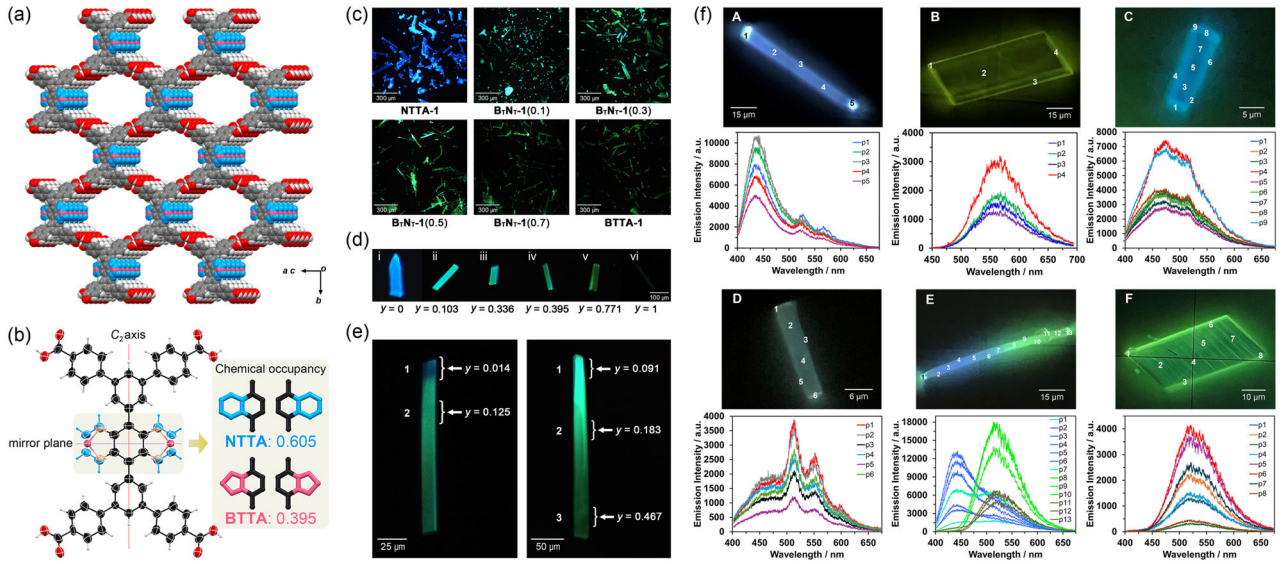

FIGURE 14 | The crystal structure and solid-state fluorescence properties of mixed HOF $\mathbf{B_TN_T}$**-1**, composed of tectons **18b** and **20**. (a) Packing diagrams of $\mathbf{B_TN_T}$**-1**. (b) Anisotropic displacement ellipsoid plot of $\mathbf{B_TN_T}$**-1** (0.3, 0.395) with 50 % probability, in which the core moieties are disordered in two structures corresponding to **BTTA** (**18b**) and **NTTA** (**20**), with occupancies of 0.395 and 0.605, respectively. (c) Fluorescence photographs of bulk crystals of **NTTA-1**, **BTTA-1**, and $\mathbf{B_TN_T}$**-1(x)** (x = 0.1, 0.3, 0.5, 0.7) HOFs, where x values show the molar fraction of BTTA in the initial solution. (d) Fluorescence photographs of single crystals whose composition ratios were determined by SCXRD. (e) Determination of composition ratio for several positions in inhomogeneous single crystals showing blue-green and light green-dark yellow by local SCXRD analysis. *y* denotes the crystallographically determined occupancy of **18b**. Emission photographs and spectra were obtained of representative single crystals of the synthesized and studied HOFs: **NTTA-1** (crystal-A), **BTTA-1**(crystal-B), and $\mathbf{B_TN_T}$**-1**(0.3): blue (crystal-C), white (crystal-D), blue-green (crystal-E), and green (crystal-F). The points on the crystal indicate the position from which the emission spectra were recorded. Reproduced with permission from ref [55]. Copyright 2024 Wiley-VCH GmbH.

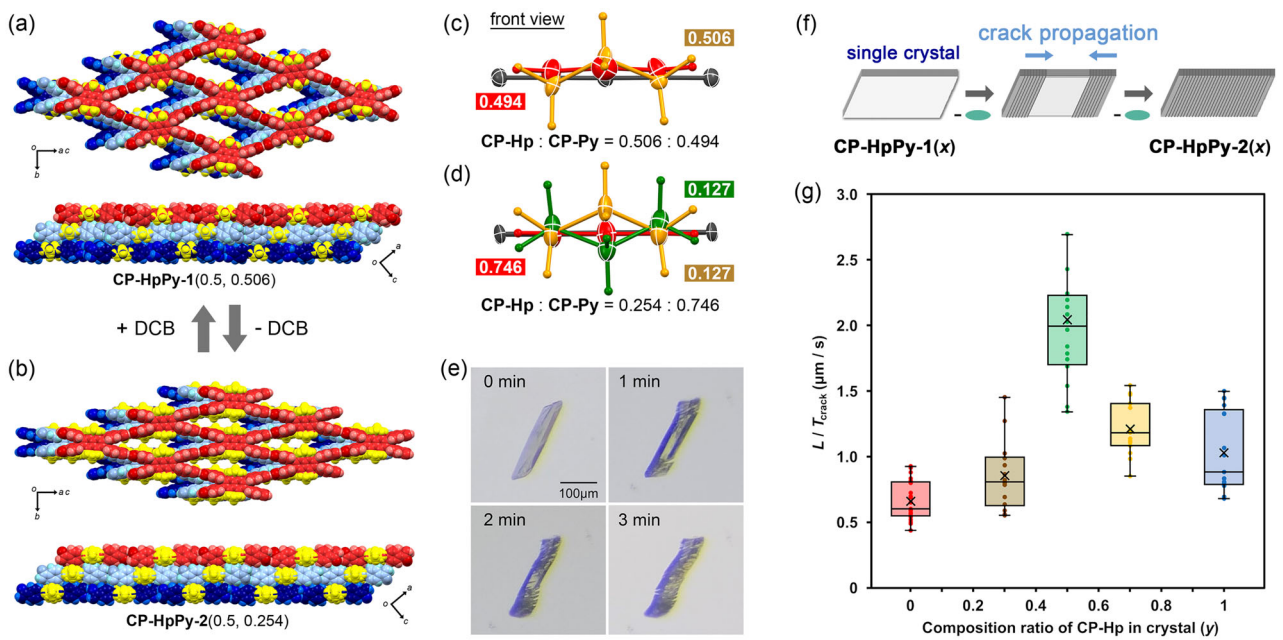

FIGURE 15 | Dynamic structural transformation of mixed HOF **CP-HpPy-1**(0.5) to **CP-HpPy-2**(0.5) composed of tectons **25** and **26**. Representative crystal structures of (a) **CP-HpPy-1**(0.5, 0.506) and (b) **CP-HpPy-2**(0.5, 0.254) revealed by SCXRD analysis, where molecules of included DCB are omitted. Disordered structure of the hydropyrene (yellow and green) and pyrene (red) core in (c) **CP-HpPy-1**(0.5, 0.506) and (d) **CP-HpPy-2**(0.5, 0.254). (e) Morphological changes of a single crystal of **CP-HpPy-1**(0.5) after wiping off bulk solvent from the surface of the crystal. (f) Cracking in a single crystal of the framework upon the structural transformation. (g) Schematic diagram for the transformation speed of **CP-Hp-1**, **CP-Py-1**, and **CP-HpPy-1**(x). The speed of **CP-Hp-1** is larger than that of **CP-Py-1**, while the speed of **CP-HpPy-1**(x) changes in a nonlinear manner depending on the composition ratio of **CP-Hp** and **CP-Py**. **CP-HpPy-1**(0.5) exhibits the maximum transformation speed. Reproduced with permission from ref [68]. Copyright 2025 Wiley-VCH GmbH.

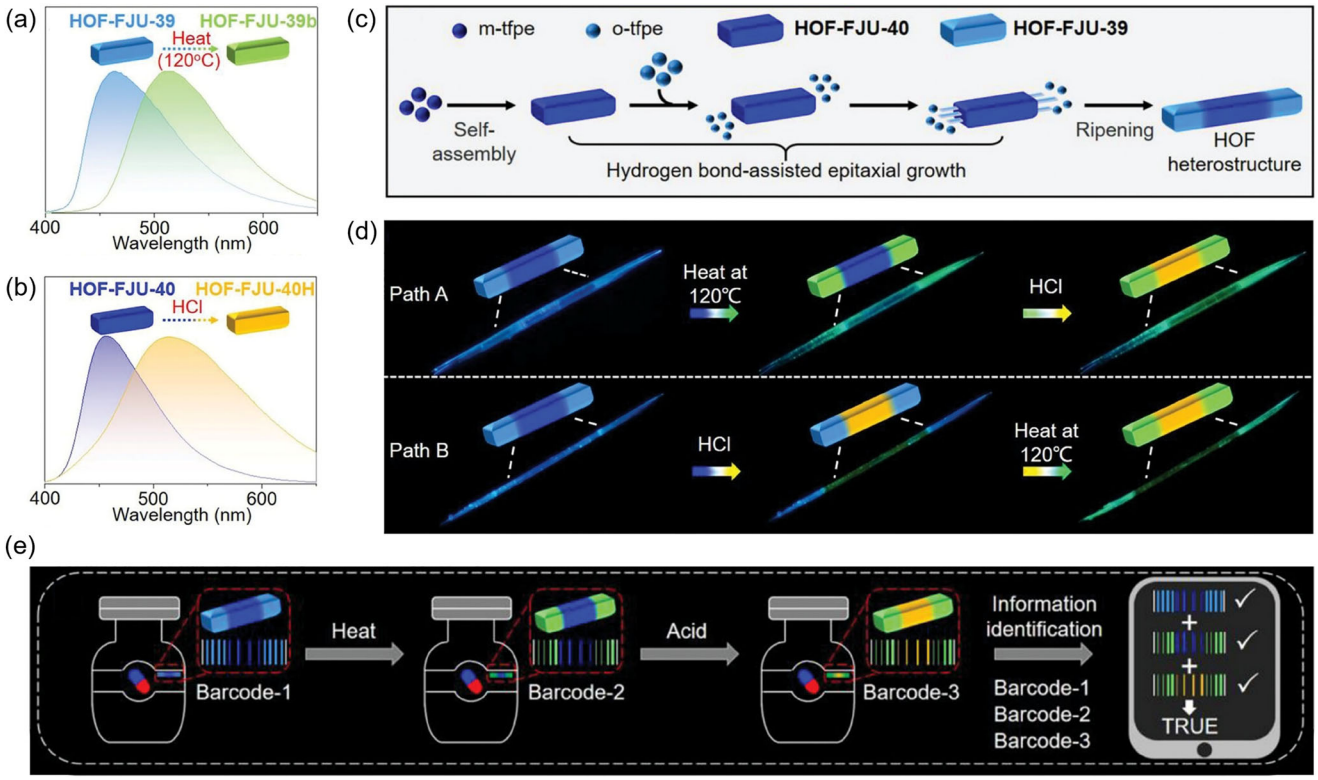

FIGURE 16 | Multi-block HOF crystals composed of tectons **68a** and **68b**. (a) PL spectra of **HOF-FJU-39** and **HOF-FJU-39b**. (b) PL spectra of **HOF-FJU-40** and **HOF-FJU-40H**. (c) Schematic illustration of the hydrogen bond-assisted epitaxial-growth process of the HOF heterostructure. (d) PL images of HOF heterostructures under thermal and acid stimulations in different orders. (e) Proof-of-concept demonstration of the smart-responsive HOF-heterostructure-based photonic barcodes for anticounterfeiting application. Reproduced with permission from ref [155]. Copyright 2023 Wiley-VCH GmbH.

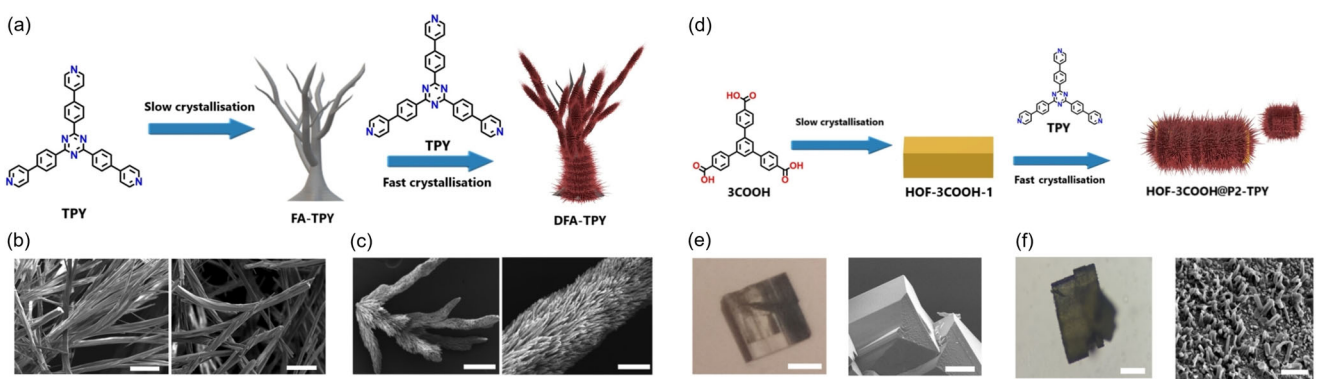

FIGURE 17 | Morphological modulation of mixed HOFs. (a) Schematic representation of the sequential crystallization of **FA-TPY** and **DFA-TPY** with tecton **4b**. SEM images of (b) **FA-TPY** and (c) **DFA-TPY**. Scale bars (from left to right): (b) 100 μm, 100 μm, (c) 100 μm, 10 μm. (d) Schematic representation of the sequential crystallization of **HOF-3COOH@P2-TPY** using tectons **2a** and **4b**. Optical (Left) and SEM (Right) images of (e) **HOF-3COOH** and (f) **HOF-3COOH@P2-TPY**. Reproduced from ref [158].

exhibit distinct responsive characters of thermochromism via the framework transformation and acidichromism via protonation, respectively, which endow the HOF heterostructures with multiple emission modes responsive to external stimuli [155]. Tetraphenylethene-based **69a** and **69b** with thiophen ring and furan ring, respectively, are integrated by an epitaxial growth method to yield monochromatic HOF heterostructures composed of **HOF-FJU-107** and **HOF-FJU-109**. The hetero HOF exhibits partial fluorescence response under heating, due to the ring-opening reaction of furan moieties [156]. Two dumbbell-shaped tectons **70** and **71** yield bulk crystals of mixed HOFs **BHJ HOFs**, showing composition-dependent fluorescence color from blue to red via white. Furthermore, sequential crystallization of the tectons gives rod-like triblock heterojunction HOFs **THJ HOFs** that act as an excellent platform for information encryption and anticounterfeit [157].

Tectons **2a** and **4b** yield three types of core–shell HOFs by rapid sequential crystallization (Figure 17). Core-shell HOFs **DFA-TPY@P2-TPY** and **P2-TPY@P2-TPY** are constructed by the single component of **4b** and exhibit different crystal morphologies. On the other hand, **HOF-3COOH@P2-TPY** is composed of two kinds of tectons, **2a** and **4b** [158]. These core-shell HOFs exhibit superhydrophobicity and trapping abilities for the capture of persistent water contaminants such as oils and microplastics.

5 | Conclusion and Perspectives

Fifteen years have passed since porous molecular crystals formed by the assembly of tectons via hydrogen bonding were redefined as "hydrogen-bonded organic frameworks" in 2011. During this time, a wide variety of constituent molecules have been synthesized, and numerous HOFs have been reported. Tectons, which feature a benzene ring as a core and incorporate three to six aryl arms bearing H-bonding groups at various positions, are one of the simplest families of tectons. PAH- and hetero-PAH-based HOFs are thermodynamically stabilized by the shape-persistent, rigid skeletons and the extensive π–π stacking between the cores. Furthermore, due to the tuned electronic states of the cores, such HOFs exhibit photoelectronic properties, which can lead to applications such as photocatalysis.

- Focusing on H-bonding functional groups that form supramolecular synthons, the DAT group was the mainstream choice for HOFs with permanent porosity in the early days. After it was demonstrated that even carboxylic acid dimers could maintain permanent porosity, numerous HOFs composed of carboxylic acid derivatives have been reported. In addition, pyrazole and pyridine have also been continuously utilized. A notable trend in recent years is applying tectons in which cyano groups are introduced as H-bonding sites. The weak H-bonding of such groups facilitates structural changes in HOFs, making it ideal for constructing open-gate or breathing-type HOFs. These HOFs are attracting significant attention as materials capable of selectively adsorbing and separating specific chemical species from mixtures of isomers and analogs of gases and volatile hydrocarbons.

- Some important concepts on HOFs have also been developed. A series of isoreticular (isostructural) HOFs can be constructed by utilizing a combination of arms with various lengths and skeletons with similar geometric structures but different properties. Isoreticular HOFs share identical geometric characteristics of their voids, allowing the series to undergo stepwise variation in pore size alone, or conversely, maintaining the same pore shape and size while altering the chemical properties of the pore surfaces. Such an isoreticular HOF library can be applied as tailor-made molecular sieves and catalysts, which is expected to grow significantly. To tune functionality and create new ones, multicomponent HOFs with non-stoichiometric mixing ratios of tectons are being actively researched. Although there are still challenges in controlling how these components mix, if this can be achieved, it will become a powerful platform for constructing a library of functional porous crystals. As mentioned in the section on cyanide-based HOFs, flexible HOFs that utilize the reversible formation and breaking of hydrogen bonds have been the subject of very active research in recent years. The correlation between their dynamic behavior and the chemical structure of the tectons has finally begun to emerge. This is a category of HOFs that is poised for further development. Currently, porous frameworks, centered on MOFs, are beginning to transition into industrial applications.

Due to their inherent characteristics, HOFs are relatively easy to synthesize as large single crystals, despite their low mechanical strength, making them an ideal platform for demonstrating various new properties and functions of porous materials. Furthermore, because they can be easily recovered, purified, and recycled, demand for them as sustainable materials is expected to grow significantly in the future.

Author Contributions

Taito Hashimoto: writing – original draft, writing – review and editing, and conceptualization. **Ichiro Hisaki:** writing – original draft, writing – review and editing, and conceptualization.

Acknowledgments

The authors acknowledge JSPS Japan for their financial support (KAKENHI: JP23H04029, JP24K01468, JP25H01672, and JP25H02042). T.H. thanks the financial support by from the Grant-in-Aid for JSPS Research Fellow (JP24KJ1655).

Conflicts of Interest

The authors declare no conflicts of interest

Data Availability Statement

The data that supports the findings of this study are available in the supplementary material of this article

References

1. Details of Nobel Prize in Chemistry 2025 can be found under https://www.nobelprize.org/prizes/chemistry/2025/summary/ (2025).

2. A. E. Smith, "The Crystal Structure of the Urea–hydrocarbon Complexes," *Acta Crystallographica* 5 (1952): 224–235, https://doi.org/10.1107/S0365110X52000629.

3. H. M. Powell and B. D. P. Wetters, "Crystallographic Examination of some Inclusion Compounds," *Chemistry & Industry (London)* 74 (1955): 256.

4. R. M. Barrer and V. H. Shanson, "Dianin's Compound as a Zeolitic Sorbent," *Journal of the Chemical Society, Chemical Communications* 12 (1976): 333, https://doi.org/10.1039/c39760000333.

5. Y. He, S. Xiang, and B. Chen, "A Microporous Hydrogen-Bonded Organic Framework for Highly Selective C_2H_2/C_2H_4 Separation at Ambient Temperature," *Journal of the American Chemical Society* 133 (2011): 14570–14573, https://doi.org/10.1021/ja2066016.

6. P. Brunet, M. Simard, and J. D. Wuest, "Molecular Tectonics. Porous Hydrogen-Bonded Networks With Unprecedented Structural Integrity," *Journal of the American Chemical Society* 119 (1997): 2737–2738, https://doi.org/10.1021/ja963905e.

7. R.-B. Lin, Y. He, P. Li, H. Wang, W. Zhou, and B. Chen, "Multifunctional Porous Hydrogen-Bonded Organic Framework Materials," *Chemical Society Reviews* 48 (2019): 1362–1389, https://doi.org/10.1039/C8CS00155C.

8. I. Hisaki, C. Xin, K. Takahashi, and T. Nakamura, "Designing Hydrogen-Bonded Organic Frameworks (HOFs) With Permanent Porosity," *Angewandte Chemie International Edition* 58 (2019): 11160–11170, https://doi.org/10.1002/anie.201902147.

9. X. Song, Y. Wang, C. Wang, et al., "Design Rules of Hydrogen-Bonded Organic Frameworks With High Chemical and Thermal Stabilities," *Journal of the American Chemical Society* 144 (2022): 10663–10687, https://doi.org/10.1021/jacs.2c02598.

10. S. Seth and S. Jhulki, "Porous Flexible Frameworks: Origins of Flexibility and Applications," *Materials Horizons* 8 (2021): 700–727, https://doi.org/10.1039/D0MH01710H.

11. J. Li and B. Chen, "Flexible Hydrogen-Bonded Organic Frameworks (HOFs): Opportunities and Challenges," *Chemical Science* 15 (2024): 9874–9892, https://doi.org/10.1039/D4SC02628D.

12. A. Pedrini, D. Marchetti, R. Pinalli, and C. Massera, "Stimuli-Responsive, Dynamic Supramolecular Organic Frameworks," *ChemPlusChem* 88 (2023): e202300383, https://doi.org/10.1002/cplu.202300383.

13. X.-J. Xi, Y. Li, F.-F. Lang, L. Xu, J. Pang, and X.-H. Bu, "Robust Porous Hydrogen-Bonded Organic Frameworks: Synthesis and Applications in Gas Adsorption and Separation," *Giant* 16 (2023): 100181, https://doi.org/10.1016/j.giant.2023.100181.

14. Z. Zhang, Y. Ye, S. Xiang, and B. Chen, "Exploring Multifunctional Hydrogen-Bonded Organic Framework Materials," *Accounts of Chemical Research* 55 (2022): 3752–3766, https://doi.org/10.1021/acs.accounts.2c00686.

15. X. Liu, G. Liu, T. Fu, et al., "Structural Design and Energy and Environmental Applications of Hydrogen-Bonded Organic Frameworks: A Systematic Review," *Advanced Science* 11 (2024): 2400101, https://doi.org/10.1002/advs.202400101.

16. H. Wang, Y. Zhang, J.-N. Shui, H. Sun, and C. Wang, "Hydrogen-Bonded Organic Framework Membranes: Emerging Nanofluidic Platforms for Gas Separation," *Chemistry—A European Journal* 31 (2025): e02541, https://doi.org/10.1002/chem.202502541.

17. C. Chen, L. Shen, H. Lin, D. Zhao, B. Li, and B. Chen, "Hydrogen-Bonded Organic Frameworks for Membrane Separation," *Chemical Society Reviews* 53 (2024): 2738–2760, https://doi.org/10.1039/D3CS00866E.

18. A. Chauhan, R. Kumar, P. Raizada, et al., "Novel Hydrogen-Bonded Organic Framework (HOF) for Highly Efficient Photocatalysis: From Structural Designs to Multifunctional Applications," *Coordination Chemistry Reviews* 535 (2025): 216634, https://doi.org/10.1016/j.ccr.2025.216634.

19. H. Yuan, J. Xiao, A.-A. Zhang, Z.-B. Fang, and T.-F. Liu, "Recent Progress of Hydrogen-Bonded Organic Framework-Based Photocatalysis," *EnergyChem* 7 (2025): 100151, https://doi.org/10.1016/j.enchem.2025.100151.

20. L. Li, T. Ma, and M. Wang, "Protein-Integrated Hydrogen-Bonded Organic Frameworks: Chemistry and Biomedical Applications," *Angewandte Chemie International Edition* 63 (2024): e202400926, https://doi.org/10.1002/anie.202400926.

21. D. Yu, H. Zhang, J. Ren, and X. Qu, "Hydrogen-Bonded Organic Frameworks: New Horizons in Biomedical Applications," *Chemical Society Reviews* 52 (2023): 7504–7523, https://doi.org/10.1039/D3CS00408B.

22. S. C. Pal, D. Mukherjee, R. Sahoo, S. Mondal, and M. C. Das, "Proton-Conducting Hydrogen-Bonded Organic Frameworks," *ACS Energy Letters* 6 (2021): 4431–4453, https://doi.org/10.1021/acsenergylett.1c02045.

23. X.-X. Xiao, K. Zheng, H.-R. Yu, F.-D. Dong, D.-Y. Hu, and R.-B. Lin, "Charge-Assisted Hydrogen-Bonded Organic Frameworks: From Crystal Engineering to Multifunctional Materials," *Chemistry–Methods* 5 (2025): e202400082, https://doi.org/10.1002/cmtd.202400082.

24. X. Zhang, L. Li, J.-X. Wang, et al., "Selective Ethane/Ethylene Separation in a Robust Microporous Hydrogen-Bonded Organic Framework," *Journal of the American Chemical Society* 142 (2020): 633–640, https://doi.org/10.1021/jacs.9b12428.

25. P. Cui and H. Zhang, "A Non-Interpenetrated Mesoporous Hydrogen-Bonded Organic Framework Constructed With 1,3,5-Tri(4-carboxyphenyl)Benzene," *Chemical Communications* 61 (2025): 2742–2745, https://doi.org/10.1039/D4CC06324D.

26. W. Yang, W. Zhou, and B. Chen, "A Flexible Microporous Hydrogen-Bonded Organic Framework," *Crystal Growth & Design* 19 (2019): 5184–5188, https://doi.org/10.1021/acs.cgd.9b00582.

27. T. Liu, B. Wang, R. He, et al., "A Novel Hydrogen-Bonded Organic Framework for the Sensing of Two Representative Organic Arsenics," *Canadian Journal of Chemistry* 98 (2020): 352–357, https://doi.org/10.1139/cjc-2019-0417.

28. Y. Zhou, L. Kan, J. F. Eubank, G. Li, L. Zhang, and Y. Liu, "Self-Assembly of Two Robust 3D Supramolecular Organic Frameworks From a Geometrically Nonplanar Molecule for High Gas Selectivity Performance," *Chemical Science* 10 (2019): 6565–6571, https://doi.org/10.1039/C9SC00290A.

29. F.-A. Guo, K. Zhou, J. Liu, H. Wang, and J. Li, "Robust Hydrogen-Bonded Organic Framework With Four-Fold Interpenetration for Adsorptive Separation of C_2H_6/C_2H_4 and Xe/Kr," *Precision Chemistry* 1 (2023): 524–529, https://doi.org/10.1021/prechem.3c00040.

30. X. Zhang, J.-X. Wang, L. Li, et al., "A Rod-Packing Hydrogen-Bonded Organic Framework With Suitable Pore Confinement for Benchmark Ethane/Ethylene Separation," *Angewandte Chemie International Edition* 60 (2021): 10304–10310, https://doi.org/10.1002/anie.202100342.

31. J.-X. Wang, X. Zhang, C. Jiang, et al., "Construction of Highly Porous and Robust Hydrogen-Bonded Organic Framework for High-Capacity Clean Energy Gas Storage," *Angewandte Chemie International Edition* 63 (2024): e202411753, https://doi.org/10.1002/anie.202411753.

32. Z. Ji, Y. Zhou, R. Krishna, M. Hong, and M. Wu, "Scalable Synthesis of Stable Hydrogen-Bonded Organic Framework for Efficient Hexafluoroethane Purification," *Angewandte Chemie International Edition* 64 (2025): e202513398, https://doi.org/10.1002/anie.202513398.

33. Z. Ji, Q. Li, Y. Zhou, R. Krishna, M. Hong, and M. Wu, "Synergistic C_2H_2 Binding Sites in Hydrogen-Bonded Supramolecular Framework for One-Step C_2H_4 Purification From Ternary C_2 Mixture," *Angewandte Chemie International Edition* 63 (2024): e202411175, https://doi.org/10.1002/anie.202411175.

34. T. Khadivjam, H. Che-Quang, T. Maris, Z. Ajoyan, A. J. Howarth, and J. D. Wuest, "Modular Construction of Porous Hydrogen-Bonded Molecular Materials From Melams," *Chemistry—A European Journal* 26 (2020): 7026–7040, https://doi.org/10.1002/chem.202000186.

35. F. Chen, Y. Cai, P. Shen, et al., "A Porous Hydrogen-Bonded Organic Framework for Sensitive and Highly Selective Fluorescence Sensing of Carcinoid Biomarkers," *Microporous and Mesoporous Materials* 361 (2023): 112759, https://doi.org/10.1016/j.micromeso.2023.112759.

36. S. Lin, P. Ke, L. Wang, et al., "Efficient Separation of Methanol-to-Olefins Products Using a Robust Polycatenated Hydrogen-Bonded Organic Framework," *Angewandte Chemie International Edition* 64 (2025): e202511773, https://doi.org/10.1002/anie.202511773.

37. Y.-L. Li, E. V. Alexandrov, Q. Yin, et al., "Record Complexity in the Polycatenation of Three Porous Hydrogen-Bonded Organic Frameworks With Stepwise Adsorption Behaviors," *Journal of the American Chemical Society* 142 (2020): 7218–7224, https://doi.org/10.1021/jacs.0c02406.

38. C. A. Halliwell, S. E. Dann, J. Ferrando-Soria, et al., "Hierarchical Assembly of a Micro- and Macroporous Hydrogen-Bonded Organic Framework With Tailored Single-Crystal Size," *Angewandte Chemie International Edition* 61 (2022): e202208677, https://doi.org/10.1002/anie.202208677.

39. Y. Li, X. Wang, H. Zhang, et al., "A Microporous Hydrogen Bonded Organic Framework for Highly Selective Separation of Carbon Dioxide Over Acetylene," *Angewandte Chemie International Edition* 62 (2023): e202311419, https://doi.org/10.1002/anie.202311419.

40. T. Fujii, K. Takaji, K. Shiga, et al., "Formation of a Hydrogen-Bonded 6^3-Network Composed of 1,2,3-Tris(4-carboxyphenyl)Benzene," *Chemistry Letters* 54 (2025): upaf111, https://doi.org/10.1093/chemle/upaf111.

41. N. Tanaka, T. Hashimoto, Y. Suzuki, R. Oketani, and I. Hisaki, "Hydrogen-Bonded Ladder Frameworks Composed of Low Symmetric Tricarboxylic Acids," *Crystal Growth & Design* 25 (2025): 1851–1859, https://doi.org/10.1021/acs.cgd.4c01697.

42. N. Murakami, R. Oketani, and I. Hisaki, "Conversion of Isolated Voids Into Channel Spaces by Modulating the Stacking Manner of Hydrogen-Bonded Ladders," *Chemistry—An Asian Journal* 20 (2025): e202401317, https://doi.org/10.1002/asia.202401317.

43. L. Gong, Y. Ye, Y. Liu, et al., "A Microporous Hydrogen-Bonded Organic Framework for Efficient Xe/Kr Separation," *ACS Applied Materials & Interfaces* 14 (2022): 19623–19628, https://doi.org/10.1021/acsami.2c04746.

44. C. Jiang, J.-X. Wang, D. Liu, et al., "Supramolecular Entanglement in a Hydrogen-Bonded Organic Framework Enables Flexible-Robust Porosity for Highly Efficient Purification of Natural Gas," *Angewandte Chemie International Edition* 63 (2024): e202404734, https://doi.org/10.1002/anie.202404734.

45. B. Yu, S. Geng, H. Wang, et al., "A Solid Transformation Into Carboxyl Dimers Based on a Robust Hydrogen-Bonded Organic Framework for Propyne/Propylene Separation," *Angewandte Chemie International Edition* 60 (2021): 25942–25948, https://doi.org/10.1002/anie.202110057.

46. F. Yuan, Y. Li, Z. Yuan, et al., "A Grafting Hydrogen-Bonded Organic Framework for Benchmark Selectivity of C_2H_2/CO_2 Separation Under Ambient Conditions," *Angewandte Chemie International Edition* 64 (2025): e202414215, https://doi.org/10.1002/anie.202414215.

47. P. Cui, Q. Zhu, F. Zhang, D. Liu, and W. Zhu, "Selective Adsorption of Polycyclic Aromatic Hydrocarbons by Isostructural Hydrogen-Bonded Organic Frameworks," *Chemical Communications* 59 (2023): 12031–12034, https://doi.org/10.1039/D3CC03131D.

48. W. Yang, J.-X. Wang, B. Yu, B. Li, H. Wang, and J. Jiang, "A Robust Hydrogen-Bonded Organic Framework With 7-Fold Interpenetration Nets and High Permanent Microporosity," *Crystal Growth & Design* 22 (2022): 1817–1823, https://doi.org/10.1021/acs.cgd.1c01382.

49. J.-X. Wang, X.-W. Gu, Y.-X. Lin, B. Li, and G. Qian, "A Novel Hydrogen-Bonded Organic Framework With Highly Permanent Porosity for Boosting Ethane/Ethylene Separation," *ACS Materials Letters* 3 (2021): 497–503, https://doi.org/10.1021/acsmaterialslett.1c00013.

50. B. Wang, R. He, L.-H. Xie, et al., "Microporous Hydrogen-Bonded Organic Framework for Highly Efficient Turn-Up Fluorescent Sensing of Aniline," *Journal of the American Chemical Society* 142 (2020): 12478–12485, https://doi.org/10.1021/jacs.0c05277.

51. Q. Chen, T. Zhang, X. Chen, et al., "Tunable Fluorescence in Two-Component Hydrogen-Bonded Organic Frameworks Based on Energy Transfer," *ACS Applied Materials & Interfaces* 14 (2022): 24509–24517, https://doi.org/10.1021/acsami.2c05897.

52. Z. Yang, A. Moriyama, R. Oketani, T. Nakamura, and I. Hisaki, "Two-Dimensional Porous Framework Assembled Through Hydrogen-bonds and Dipole-Dipole Interactions," *Chemistry Letters* 50 (2021): 1909–1912, https://doi.org/10.1246/cl.210465.

53. Z. Yang, A. Saeki, A. Inoue, et al., "Slip-Stacking of Benzothiadiazole Can Provide a Robust Structural Motif for Porous Hydrogen-Bonded Organic Frameworks," *Crystal Growth & Design* 22 (2022): 4472–4479, https://doi.org/10.1021/acs.cgd.2c00420.

54. P. Cui, E. Svensson Grape, P. R. Spackman, et al., "An Expandable Hydrogen-Bonded Organic Framework Characterized by Three-Dimensional Electron Diffraction," *Journal of the American Chemical Society* 142 (2020): 12743–12750, https://doi.org/10.1021/jacs.0c04885.

55. T. Hashimoto, M. de la Hoz Tomás, R. Oketani, et al., "Single Crystalline, Non-Stoichiometric Hydrogen-Bonded Organic Frameworks Showing Versatile Fluorescence Depending on Composition Ratios and Distributions," *Angewandte Chemie International Edition* 64 (2025): e202419992, https://doi.org/10.1002/anie.202419992.

56. Y.-B. Wang, Y.-X. Lin, J.-X. Wang, et al., "A Microporous Hydrogen-Bonded Organic Framework With Alkynyl Sites for Highly Efficient Propane/Propylene Separation," *Journal of the American Chemical Society* 147 (2025): 24403–24412, https://doi.org/10.1021/jacs.5c02924.

57. Y.-B. Wang, T.-F. Zhang, Y.-X. Lin, et al., "A Novel Microporous Hydrogen-Bonded Organic Framework With Electron-Rich Alkynyl Groups for Highly Efficient C_2H_6/C_2H_4 Separation," *Journal of Materials Chemistry A* 12 (2024): 25812–25819, https://doi.org/10.1039/D4TA04528A.

58. Y. Murata, T. Hashimoto, R. Oketani, et al., "A Hydrogen-Bonded Organic Framework Possessing One-Dimensional Wide Channels Surrounded by the Naphthalenediimide Plane," *Chemical Science* 17 (2026): 2811–2817, https://doi.org/10.1039/D5SC07488F.

59. Q. Yin, P. Zhao, R.-J. Sa, et al., "An Ultra-Robust and Crystalline Redeemable Hydrogen-Bonded Organic Framework for Synergistic Chemo-Photodynamic Therapy," *Angewandte Chemie International Edition* 57 (2018): 7691–7696, https://doi.org/10.1002/anie.201800354.

60. X. Yu Gao, Y. Wang, E. Wu, et al., "Multivariate Hydrogen-Bonded Organic Frameworks With Tunable Permanent Porosities for Capture of a Mustard Gas Simulant," *Angewandte Chemie International Edition* 62 (2023): e202312393, https://doi.org/10.1002/anie.202312393.

61. Y. Zou, H.-X. Liu, L. Cai, et al., "Strategy to Efficient Photodynamic Therapy for Antibacterium: Donor-Acceptor Structure in Hydrogen-Bonded Organic Framework," *Advanced Materials* 36 (2024): 2406026, https://doi.org/10.1002/adma.202406026.

62. B. Wang, X.-L. Lv, J. Lv, et al., "A Novel Mesoporous Hydrogen-Bonded Organic Framework With High Porosity and Stability," *Chemical Communications* 56 (2020): 66–69, https://doi.org/10.1039/C9CC07802A.

63. X. Song, Y. Wang, C. Wang, et al., "Self-Healing Hydrogen-Bonded Organic Frameworks for Low-Concentration Ammonia Capture," *Journal of the American Chemical Society* 146 (2024): 627–634, https://doi.org/10.1021/jacs.3c10492.

64. J. Liu, G. Mo, X. Gao, et al., "Enzyme-Inspired Hydrogen-Bonded Organic Frameworks for Synergistic Capture, Detection, and Degradation of Nerve Agent Simulants," *Advanced Science* 13 (2026): e19971, https://doi.org/10.1002/advs.202519971.

65. L. He, Y. Li, L. Li, et al., "A Microporous Hydrogen-Bonded Organic Framework With Open Pyrene Sites Isolated by Hydrogen-Bonded Helical Chains for Efficient Separation of Xenon and Krypton," *Angewandte Chemie International Edition* 64 (2025): e202418917, https://doi.org/10.1002/anie.202418917.

66. T. Hashimoto, R. Oketani, A. Inoue, et al., "Statically and Dynamically Flexible Hydrogen-Bonded Frameworks Based on 4,5,9,10-Tetrakis(4-carboxyphenyl)Pyrene," *Chemical Communications* 59 (2023): 7224–7227, https://doi.org/10.1039/D3CC01877F.

67. T. Hashimoto, R. Oketani, M. Nobuoka, S. Seki, and I. Hisaki, "Single Crystalline, Non-Stoichiometric Cocrystals of Hydrogen-Bonded Organic Frameworks," *Angewandte Chemie International Edition* 62 (2023): e202215836, https://doi.org/10.1002/anie.202215836.

68. T. Hashimoto, R. Oketani, and I. Hisaki, "Composition Dependent Dynamic Behaviors of Non-Stoichiometric Cocrystalline Hydrogen-Bonded Organic Frameworks," *Small* 21 (2025): e08763, https://doi.org/10.1002/smll.202508763.

69. M. Hu, C. Wu, S. Feng, and J. Hua, "A High Crystalline Perylene-Based Hydrogen-Bonded Organic Framework for Enhanced Photocatalytic H_2O_2 Evolution," *Molecules* 28 (2023): 6850, https://doi.org/10.3390/molecules28196850.

70. L. Wang, L. Yang, L. Gong, et al., "Constructing Redox-Active Microporous Hydrogen-Bonded Organic Framework by Imide-Functionalization: Photochromism, Electrochromism, and Selective Adsorption of C_2H_2 Over CO_2," *Chemical Engineering Journal* 383 (2020): 123117, https://doi.org/10.1016/j.cej.2019.123117.

71. Y. Wu, X. Mao, M. Zhang, et al., "2D Molecular Sheets of Hydrogen-Bonded Organic Frameworks for Ultrastable Sodium-Ion Storage," *Advanced Materials* 33 (2021): 2106079, https://doi.org/10.1002/adma.202106079.

72. I. Hisaki, Y. Suzuki, E. Gomez, et al., "Acid Responsive Hydrogen-Bonded Organic Frameworks," *Journal of the American Chemical Society* 141 (2019): 2111–2121, https://doi.org/10.1021/jacs.8b12124.

73. I. Hisaki, Q. Ji, K. Takahashi, N. Tohnai, and T. Nakamura, "Positional Effects of Annelated Pyrazine Rings on Structure and Stability of Hydrogen-Bonded Frameworks of Hexaazatrinaphthylene Derivatives," *Crystal Growth & Design* 20 (2020): 3190–3198, https://doi.org/10.1021/acs.cgd.0c00055.

74. H. Kubo, S. Konishi, R. Oketani, T. Hayashi, and I. Hisaki, "Transition Behaviors of Isostructural Hydrogen-Bonded Frameworks Composed of Naphthalene, Quinoxaline, and Pyrazinopyrazine Derivatives," *Chemistry—A European Journal* 30 (2024): e202401645, https://doi.org/10.1002/chem.202401645.

75. Q. Ji, K. Takahashi, S. Noro, et al., "A Hydrogen-Bonded Organic Framework Based on Pyrazinopyrazine," *Crystal Growth & Design* 21 (2021): 4656–4664, https://doi.org/10.1021/acs.cgd.1c00506.

76. I. Hisaki, N. Q. Emilya Affendy, and N. Tohnai, "Precise Elucidations of Stacking Manners of Hydrogen-Bonded Two-Dimensional Organic Frameworks Composed of X-Shaped π-Conjugated Systems," *Crystal Engineering Communications* 19 (2017): 4892–4898, https://doi.org/10.1039/C7CE00183E.

77. H. Kubo, R. Oketani, and I. Hisaki, "Quasi Single-Crystalline Transformation of Porous Frameworks Accompanied by Interlayer Rearrangements of Hydrogen Bonds," *Chemical Communications* 57 (2021): 8568–8571, https://doi.org/10.1039/D1CC03287A.

78. H. Kubo, R. Oketani, and I. Hisaki, "Desolvation-Induced Network Reformation and Cracking in the Single Crystals of Hydrogen-Bonded Frameworks Composed of Tetraazaanthraquinone and Anthraquinone Derivatives," *Angewandte Chemie International Edition* 64 (2025): e202510977, https://doi.org/10.1002/anie.202510977.

79. X.-Y. Gao, Y.-L. Li, T.-F. Liu, X.-S. Huang, and R. Cao, "Single-Crystal-to-Single-Crystal Transformation of Tetrathiafulvalene-Based Hydrogen-Bonded Organic Frameworks," *CrystEngComm* 23 (2021): 4743–4747, https://doi.org/10.1039/D1CE00519G.

80. K. O. Kirlikovali, S. Goswami, M. R. Mian, et al., "An Electrically Conductive Tetrathiafulvalene-Based Hydrogen-Bonded Organic Framework," *ACS Materials Letters* 4 (2022): 128–135, https://doi.org/10.1021/acsmaterialslett.1c00628.

81. L. Li, F. Xiang, Y. Li, et al., "Optimizing Propylene/Propane Sieving Separation Through Gate-Pressure Control Within a Flexible Organic Framework," *Angewandte Chemie International Edition* 64 (2025): e202419047, https://doi.org/10.1002/anie.202419047.

82. Y. Suzuki, N. Tohnai, A. Saeki, and I. Hisaki, "Hydrogen-Bonded Organic Frameworks of Twisted Polycyclic Aromatic Hydrocarbon," *Chemical Communications* 56 (2020): 13369–13372, https://doi.org/10.1039/D0CC06081J.

83. Y. Suzuki, M. Yamaguchi, R. Oketani, and I. Hisaki, "Isomeric Effect of Naphthyl Spacers on Structures and Properties of Isostructural Porous Crystalline Frameworks," *Materials Chemistry Frontiers* 7 (2023): 106–116, https://doi.org/10.1039/D2QM01091G.

84. I. Hisaki, N. Ikenaka, E. Gomez, B. Cohen, N. Tohnai, and A. Douhal, "Hexaazatriphenylene-Based Hydrogen-Bonded Organic Framework With Permanent Porosity and Single-Crystallinity," *Chemistry—A European Journal* 23 (2017): 11611–11619, https://doi.org/10.1002/chem.201701893.

85. I. Hisaki, Y. Suzuki, E. Gomez, B. Cohen, N. Tohnai, and A. Douhal, "Docking Strategy To Construct Thermostable, Single-Crystalline, Hydrogen-Bonded Organic Framework With High Surface Area," *Angewandte Chemie International Edition* 57 (2018): 12650–12655, https://doi.org/10.1002/anie.201805472.

86. Y. Suzuki, M. Gutiérrez, S. Tanaka, et al., "Construction of Isostructural Hydrogen-Bonded Organic Frameworks: Limitations and Possibilities of Pore Expansion," *Chemical Science* 12 (2021): 9607–9618, https://doi.org/10.1039/D1SC02690A.

87. K. I. Shivakumar, S. Noro, Y. Yamaguchi, et al., "A Hydrogen-Bonded Organic Framework Based on Redox-Active Tri(dithiolylidene)Cyclohexanetrione," *Chemical Communications* 57 (2021): 1157–1160, https://doi.org/10.1039/D0CC07776C.

88. Z. Yang, T. Hashimoto, R. Oketani, T. Nakamura, and I. Hisaki, "Geometrically Mismatched Hydrogen-Bonded Framework Composed of Tetratopic Carboxylic Acid," *Chemistry—A European Journal* 28 (2022): e202201571.

89. B.-T. Liu, X.-H. Pan, D.-Y. Zhang, et al., "Construction of Function-Oriented Core–Shell Nanostructures in Hydrogen-Bonded Organic Frameworks for Near-Infrared-Responsive Bacterial Inhibition," *Angewandte Chemie International Edition* 60 (2021): 25701–25707.

90. Z. Yuan, X. Jiang, L. Chen, et al., "Sticked-Layer Strategy to a Flexible-Robust Hydrogen-Bonded Organic Framework for Efficient C_2H_2/CO_2 Separation," *CCS Chemistry* 6 (2023): 663–671, https://doi.org/10.31635/ccschem.023.202302840.

91. Z. Yuan, L. Chen, X. Zhou, et al., "Hydrogen-Bonded Organic Framework With Tailored Pores Prepared by Enlarging the Core Size for High-Performance Xe/Kr Separation," *Journal of Materials Chemistry A* 11 (2023): 21857–21863, https://doi.org/10.1039/D3TA04738E.

92. L. Zhao, Y. Tu, F. Luo, G. Liu, and C. Fan, "Hydrogen-Bonded Organic Framework for Fluorescence-Guided Toluene/Methylcyclohexane Separation," *ACS Applied Polymer Materials* 7 (2025): 13447–13454, https://doi.org/10.1021/acsapm.5c01530.

93. S. Lin, Y. Liang, P. Ke, et al., "Efficient Methane Purification Using a Robust and Recoverable Hydrogen-Bonded Organic Framework," *Angewandte Chemie International Edition* 64 (2025): e202500970, https://doi.org/10.1002/anie.202500970.

94. F. Yuan, G. Han, Y. Li, et al., "Flexible Hydrogen-Bonded Organic Framework With Anthracene Core for Recognition of Benzene over Cyclohexane," *Angewandte Chemie International Edition* 64 (2025): e202513288, https://doi.org/10.1002/anie.202513288.

95. Y. Chen, Y. Yang, Y. Wang, et al., "Ultramicroporous Hydrogen-Bonded Organic Framework Material With a Thermoregulatory Gating Effect for Record Propylene Separation," *Journal of the American Chemical Society* 144 (2022): 17033–17040, https://doi.org/10.1021/jacs.2c06585.

96. Y. Yang, L. Li, R.-B. Lin, et al., "Ethylene/Ethane Separation in a Stable Hydrogen-Bonded Organic Framework Through a Gating Mechanism," *Nature Chemistry* 13 (2021): 933–939, https://doi.org/10.1038/s41557-021-00740-z.

97. Q. Huang, K. Otake, and S. Kitagawa, "A Nitro-Modified Luminescent Hydrogen-Bonded Organic Framework for Non-Contact and High-Contrast Sensing of Aromatic Amines," *Angewandte Chemie International Edition* 62 (2023): e202310225, https://doi.org/10.1002/anie.202310225.

98. L. Chen, Z. Yuan, H. Zhang, et al., "A Flexible Hydrogen-Bonded Organic Framework Constructed From a Tetrabenzaldehyde With a Carbazole N−H Binding Site for the Highly Selective Recognition and Separation of Acetone," *Angewandte Chemie International Edition* 61 (2022): e202213959, https://doi.org/10.1002/anie.202213959.

99. L. Li, X. Zhang, X. Lian, et al., "Flue Gas Desulfurization and SO_2 Recovery Within a Flexible Hydrogen-Bonded Organic Framework," *Nature Chemistry* 17 (2025): 727–733, https://doi.org/10.1038/s41557-025-01744-9.

100. C. E. Shields, X. Wang, T. Fellowes, et al., "Experimental Confirmation of a Predicted Porous Hydrogen-Bonded Organic Framework," *Angewandte Chemie International Edition* 62 (2023): e202303167, https://doi.org/10.1002/anie.202303167.

101. R. Zhang, H. Daglar, C. Tang, et al., "Balancing Volumetric and Gravimetric Capacity for Hydrogen in Supramolecular Crystals," *Nature*

Chemistry 16 (2024): 1982–1988, https://doi.org/10.1038/s41557-024-01622-w.

102. R. Zhang, C. Tang, S. Yang, et al., "Double-Walled Mesoporous Hydrogen-Bonded Organic Frameworks With High Methane Storage Capacity," *Journal of the American Chemical Society* 147 (2025): 16412–16419, https://doi.org/10.1021/jacs.5c02705.

103. Q. Yin, E. V. Alexandrov, D.-H. Si, et al., "Metallization-Prompted Robust Porphyrin-Based Hydrogen-Bonded Organic Frameworks for Photocatalytic CO_2 Reduction," *Angewandte Chemie International Edition* 61 (2022): e202115854, https://doi.org/10.1002/anie.202115854.

104. Y. Wang, D. Liu, J. Yin, et al., "An Ultrafast Responsive NO_2 Gas Sensor Based on a Hydrogen-Bonded Organic Framework Material," *Chemical Communications* 56 (2020): 703–706, https://doi.org/10.1039/C9CC09171H.

105. C. Wang, X. Song, Y. Wang, et al., "A Solution-Processable Porphyrin-Based Hydrogen-Bonded Organic Framework for Photoelectrochemical Sensing of Carbon Dioxide," *Angewandte Chemie International Edition* 62 (2023): e202311482, https://doi.org/10.1002/anie.202311482.

106. Y.-J. Hou, S. Fang, X.-Y. Zhang, et al., "Tetrazolyl Porphyrin-Based Hydrogen-Bonded Organic Frameworks: Active Sites-Mediated Host-Guest Synergy for Advanced Antimicrobial Applications," *ACS Applied Materials & Interfaces* 14 (2022): 49875–49885, https://doi.org/10.1021/acsami.2c15869.

107. L. Ma, Y. Xie, R. S. H. Khoo, et al., "An Adaptive Hydrogen-Bonded Organic Framework for the Exclusive Recognition of p-Xylene," *Chemistry—A European Journal* 28 (2022): e202104269, https://doi.org/10.1002/chem.202104269.

108. S. Ouyang, C. Chen, P. Lin, et al., "Hydrogen-Bonded Organic Frameworks Chelated Manganese for Precise Magnetic Resonance Imaging Diagnosis of Cancers," *Nano Letters* 23 (2023): 8628–8636, https://doi.org/10.1021/acs.nanolett.3c02466.

109. H. Park, K. H. Oh, J. H. Lee, et al., "Axial Coordination-Assisted Interwoven Isomerism in 3D Hydrogen-Bonded Organic Frameworks for Efficient Natural Gas Purification," *Journal of Materials Chemistry A* 12 (2024): 26197–26204, https://doi.org/10.1039/D4TA04918G.

110. X. Chen, K. Takahashi, K. Kokado, T. Nakamura, and I. Hisaki, "A Proton Conductive Hydrogen-Bonded Framework Incorporating 18-Crown-6-Ether and Dicarboxy- o -terphenyl Moieties," *Materials Advances* 2 (2021): 5639–5644, https://doi.org/10.1039/D1MA00411E.

111. X. Chen, R.-K. Huang, K. Takahashi, S. Noro, T. Nakamura, and I. Hisaki, "A Proton Conductive Porous Framework of an 18-Crown-6-Ether Derivative Networked by Rigid Hydrogen Bonding Modules," *Angewandte Chemie International Edition* 61 (2022): e202211686, https://doi.org/10.1002/anie.202211686.

112. I. Hisaki, S. Nakagawa, N. Ikenaka, et al., "A Series of Layered Assemblies of Hydrogen-Bonded, Hexagonal Networks of $_3$ -Symmetric π-Conjugated Molecules: A Potential Motif of Porous Organic Materials," *Journal of the American Chemical Society* 138 (2016): 6617–6628, https://doi.org/10.1021/jacs.6b02968.

113. H. Yoshimura, R. Oketani, M. Naruoka, N. Tohnai, and I. Hisaki, "A Hydrogen-Bonded, Hexagonally Networked, Layered Framework With Large Aperture Designed by Structural Synchronization of a Macrocycle and Supramolecular Synthon," *Precision Chemistry* 2 (2024): 221–228, https://doi.org/10.1021/prechem.4c00019.

114. Y. Kanetada, R. Oketani, T. Sasaki, K. Ichiyanagi, and I. Hisaki, "Hydrogen-Bonded Framework with Low-Density Hexagonal Network Structure Formed by Diethynylterphenyl-Bridged Macrocyclic Hexacarboxylic Acid," *Asian Journal of Organic Chemistry* 14 (2025): e202500288, https://doi.org/10.1002/ajoc.202500288.

115. Q. Zhu, J. Johal, D. E. Widdowson, et al., "Analogy Powered by Prediction and Structural Invariants: Computationally Led Discovery of a Mesoporous Hydrogen-Bonded Organic Cage Crystal," *Journal of the American Chemical Society* 144 (2022): 9893–9901, https://doi.org/10.1021/jacs.2c02653.

116. Q. Zhu, L. Wei, C. Zhao, et al., "Soft Hydrogen-Bonded Organic Frameworks Constructed Using a Flexible Organic Cage Hinge," *Journal of the American Chemical Society* 145 (2023): 23352–23360, https://doi.org/10.1021/jacs.3c09246.

117. J.-Q. Zhao, L.-L. Mao, G.-H. Zhang, et al., "A Polycatenated Hydrogen-Bonded Organic Framework Based on Embraced Macrocyclic Building Blocks for Fluorescence Detection of Nitrobenzene in Water," *Journal of Materials Chemistry A* 11 (2023): 4672–4678, https://doi.org/10.1039/D2TA09379K.

118. D. Wang and Y. Zhao, "Rigid-Flexible Hybrid Porous Molecular Crystals With Guest-Induced Reversible Crystallinity," *Angewandte Chemie International Edition* 62 (2023): e202217903, https://doi.org/10.1002/anie.202217903.

119. J. R. Pathan, X. Pang, S. C. Olsen, et al., "Macrocycle Side Chain Crowding Enables Tunable Curvature From Planar to Wrinkled and Wavy Hydrogen-Bonded Sheets," *Journal of the American Chemical Society* 147 (2025): 28570–28576, https://doi.org/10.1021/jacs.5c07383.

120. Y. Suzuki, N. Tohnai, and I. Hisaki, "Triaxially Woven Hydrogen-Bonded Chicken Wires of a Tetrakis(carboxybiphenyl)Ethene," *Chemistry—A European Journal* 26 (2020): 17056–17062, https://doi.org/10.1002/chem.202002546.

121. M. Yamaguchi, M. D. L. H. Tomás, A. Fujiwara, et al., "An Expanded Hydrogen-Bonded Organic Framework Formed by a Tetrakis(terphenyl)Ethene Derivative," *Bulletin of the Chemical Society of Japan* 97 (2024): uoae004, https://doi.org/10.1093/bulcsj/uoae004.

122. Q. Huang, W. Li, Z. Yang, et al., "Achieving Bright Mechanoluminescence in a Hydrogen-Bonded Organic Framework by Polar Molecular Rotor Incorporation," *CCS Chemistry* 4 (2021): 1643–1653, https://doi.org/10.31635/ccschem.021.202100968.

123. Q. Huang, X. Chen, W. Li, et al., "Local Dynamics in a Hydrogen-Bonded Organic Framework for Adaptive Guest Accommodation With Programmable Luminescence," *Chemistry* 9 (2023): 1241–1254, https://doi.org/10.1016/j.chempr.2023.01.013.

124. Y. Shi, Y. Ding, W. Tao, and P. Wei, "Solvent-Triggered Fast and Visible Switching Between Cage- and Channel-Type Hydrogen-Bonded Organic Frameworks," *ACS Applied Materials & Interfaces* 14 (2022): 36071–36078, https://doi.org/10.1021/acsami.2c11800.

125. Y. Lv, Z. Xiong, Y. Li, et al., "Framework-Shrinkage-Induced Wavelength-Switchable Lasing From a Single Hydrogen-Bonded Organic Framework Microcrystal," *The Journal of Physical Chemistry Letters* 13 (2022): 130–135, https://doi.org/10.1021/acs.jpclett.1c03855.

126. Q. Huang, W. Li, Z. Mao, et al., "Dynamic Molecular Weaving in a Two-Dimensional Hydrogen-Bonded Organic Framework," *Chemistry* 7 (2021): 1321–1332, https://doi.org/10.1016/j.chempr.2021.02.017.

127. Q. Huang, W. Li, Z. Mao, et al., "An Exceptionally Flexible Hydrogen-Bonded Organic Framework With Large-Scale Void Regulation and Adaptive Guest Accommodation Abilities," *Nature Communications* 10 (2019): 3074, https://doi.org/10.1038/s41467-019-10575-5.

128. S.-C. Wang, Q.-S. Zhang, Z. Wang, et al., "Tetraphenylethylene-Based Hydrogen-Bonded Organic Frameworks (HOFs) With Brilliant Fluorescence," *Angewandte Chemie International Edition* 62 (2023): e202315382, https://doi.org/10.1002/anie.202315382.

129. Y. Shi, S. Wang, W. Tao, et al., "Multiple yet Switchable Hydrogen-Bonded Organic Frameworks With White-Light Emission," *Nature Communications* 13 (2022): 1882, https://doi.org/10.1038/s41467-022-29565-1.

130. H. Li, C. Chen, Q. Li, et al., "An Ultra-Stable Supramolecular Framework Based on Consecutive Side-by-Side Hydrogen Bonds for One-Step C_2H_4/C_2H_6 Separation," *Angewandte Chemie International Edition* 63 (2024): e202401754, https://doi.org/10.1002/anie.202401754.

131. L. Zhang, Y.-T. Luo, S.-J. Xiao, et al., "The Construction of a Stable Hydrogen-Bonded Organic Framework for The Photocatalytic Reduction and Removal of Uranium," *Chemical Communications* 60 (2024): 3583–3586, https://doi.org/10.1039/D4CC00438H.

132. W. Yang, J. Wang, H. Wang, Z. Bao, J. C.-G. Zhao, and B. Chen, "Highly Interpenetrated Robust Microporous Hydrogen-Bonded Organic Framework for Gas Separation," *Crystal Growth & Design* 17 (2017): 6132–6137, https://doi.org/10.1021/acs.cgd.7b01322.

133. J. Gao, Y. Cai, X. Qian, et al., "A Microporous Hydrogen-Bonded Organic Framework for the Efficient Capture and Purification of Propylene," *Angewandte Chemie International Edition* 60 (2021): 20400–20406, https://doi.org/10.1002/anie.202106665.

134. Y. Zhou, C. Chen, R. Krishna, Z. Ji, D. Yuan, and M. Wu, "Tuning Pore Polarization to Boost Ethane/Ethylene Separation Performance in Hydrogen-Bonded Organic Frameworks," *Angewandte Chemie International Edition* 62 (2023): e202305041, https://doi.org/10.1002/anie.202305041.

135. Y.-M. Liu, B.-T. Liu, Y.-L. Li, J.-L. Li, T.-F. Liu, and L. Cai, "A Stable Pyridone-Based Hydrogen-Bonded Organic Framework for Electrochemical Detection of Dopamine," *Materials Chemistry Frontiers* 8 (2024): 1128–1133, https://doi.org/10.1039/D3QM01124K.

136. Y. Shang, L. Ma, Z. Kang, et al., "Integrated Monomer Synthesis and Framework Assembly: Achieving Isoreticular Modulation of Hydrogen-Bonded Organic Frameworks," *Angewandte Chemie International Edition* 64 (2025): e202416966, https://doi.org/10.1002/anie.202416966.

137. Y. Han, T. Zhang, X. Chen, et al., "Guest-Regulated Luminescence and Force-Stimuli Response of a Hydrogen-Bonded Organic Framework," *ACS Applied Materials & Interfaces* 13 (2021): 32270–32277, https://doi.org/10.1021/acsami.1c08316.

138. S. Feng, Y. Shang, Z. Wang, et al., "Fabrication of a Hydrogen-Bonded Organic Framework Membrane Through Solution Processing for Pressure-Regulated Gas Separation," *Angewandte Chemie International Edition* 59 (2020): 3840–3845, https://doi.org/10.1002/anie.201914548.

139. A. Pulido, L. Chen, T. Kaczorowski, et al., "Functional Materials Discovery Using Energy–Structure–Function Maps," *Nature* 543 (2017): 657–664, https://doi.org/10.1038/nature21419.

140. T. Hashimoto, M. de la Hoz Tomás, R. Oketani, B. Cohen, A. Douhal, and I. Hisaki, "Layer Sliding-Induced Fluorescence Changes in a Flexible Hydrogen-Bonded Organic Framework," *Chemistry—A European Journal* 31 (2025): e02078, https://doi.org/10.1002/chem.202502078.

141. M. Mastalerz and I. M. Oppel, "Rational Construction of an Extrinsic Porous Molecular Crystal With an Extraordinary High Specific Surface Area," *Angewandte Chemie International Edition* 51 (2012): 5252–5255, https://doi.org/10.1002/anie.201201174.

142. M.-Z. Zhuo, X.-Y. Yan, Z.-H. Yang, Z.-Y. Chen, X.-H. Wang, and M.-X. Wu, "Hydrogen-Bonded Organic Frameworks Leveraging Lewis Basic Motifs for High-Capacity Iodine Capture," *Chemical Communications* 61 (2025): 16416–16419, https://doi.org/10.1039/D5CC03745J.

143. L. Hou, C. Shan, Y. Song, et al., "Highly Stable Single Crystals of Three-Dimensional Porous Oligomer Frameworks Synthesized Under Kinetic Conditions," *Angewandte Chemie International Edition* 60 (2021): 14664–14670, https://doi.org/10.1002/anie.202103729.

144. J. Huang, Y. Li, H. Zhang, et al., "A Microporous Hydrogen-Bonded Organic Framework Based on Hydrogen-Bonding Tetramers for Efficient Xe/Kr Separation," *Angewandte Chemie International Edition* 62 (2023): e202315987, https://doi.org/10.1002/anie.202315987.

145. J. Huang, H. Chen, Y. Li, et al., "Reticular Syntheses of Hydrogen-Bonded Organic Frameworks Based on Pyrazole Tetramers With Tunable Electrostatic Potential for Enhanced C_2H_2/CO_2 Separation," *Separation and Purification Technology* 351 (2024): 128066, https://doi.org/10.1016/j.seppur.2024.128066.

146. C. S. Diercks, Y. Liu, K. E. Cordova, and O. M. Yaghi, "The Role of Reticular Chemistry in The Design of CO_2 Reduction Catalysts," *Nature Materials* 17 (2018): 301–307, https://doi.org/10.1038/s41563-018-0033-5.

147. M. J. Kalmutzki, N. Hanikel, and O. M. Yaghi, "Secondary Building Units as the Turning Point in the Development of the Reticular Chemistry of MOFs," *Science Advances* 4 (2018): eaat9180, https://doi.org/10.1126/sciadv.aat9180.

148. O. M. Yaghi, M. J. Kalmutzki, and C. S. Diercks, *Introduction to Reticular Chemistry: Metal-Organic Frameworks and Covalent Organic Frameworks* (Wiley, 2019), https://doi.org/10.1002/9783527821099.

149. M. Eddaoudi, J. Kim, N. Rosi, et al., "Systematic Design of Pore Size and Functionality in Isoreticular MOFs and Their Application in Methane Storage," 295 (2002): 469–472, https://doi.org/10.1126/science.1067208.

150. E. L. Spitler, J. W. Colson, F. J. Uribe-Romo, et al., "Lattice Expansion of Highly Oriented 2D Phthalocyanine Covalent Organic Framework Films," *Angewandte Chemie International Edition* 51 (2012): 2623–2627, https://doi.org/10.1002/anie.201107070.

151. H. Furukawa, U. Müller, and O. M. Yaghi, ""Heterogeneity Within Order" in Metal–Organic Frameworks," *Angewandte Chemie International Edition* 54 (2015): 3417–3430, https://doi.org/10.1002/anie.201410252.

152. R. L. Li, A. Yang, N. C. Flanders, M. T. Yeung, D. T. Sheppard, and W. R. Dichtel, "Two-Dimensional Covalent Organic Framework Solid Solutions," *Journal of the American Chemical Society* 143 (2021): 7081–7087, https://doi.org/10.1021/jacs.1c01683.

153. H. Zhao, B. Fan, G. Liu, X. Liu, and P. Xue, "Recent Advances in Non-stoichiometric Multicomponent Hydrogen-Bonded Organic Frameworks," *Chemical Communications* 62 (2026): 71–82, https://doi.org/10.1039/D5CC05040E.

154. S. Liu, L. Li, X.-Y. Gao, R. Cao, Y.-B. Zhang, and T.-F. Liu, "Multivariate Hydrogen-Bonded Organic Frameworks for Optimum Atmospheric Water Harvesting," *ACS Central Science* 11 (2025): 1984–1992, https://doi.org/10.1021/acscentsci.5c01233.

155. Y. Lv, J. Liang, Z. Xiong, et al., "Smart-Responsive HOF Heterostructures With Multiple Spatial-Resolved Emission Modes Toward Photonic Security Platform," *Advanced Materials* 36 (2024): 2309130, https://doi.org/10.1002/adma.202309130.

156. Y. Lv, X. Liu, J. Liang, et al., "Monochromatic Responsive HOF Heterostructures via VIA-Group-Based Framework Hybridization for Fully-Covert Photonic Barcode," *Advanced Materials* 37 (2025): 2420486, https://doi.org/10.1002/adma.202420486.

157. H. Zhao, S. Hu, M. Liang, and P. Xue, "Heterostructure of Hydrogen-Bonded Organic Frameworks for White Light Emission and Information Encryption," *Advanced Optical Materials* 13 (2025): 2402321, https://doi.org/10.1002/adom.202402321.

158. C. A. Halliwell, K. Jolley, K. Yendall, M. R. J. Elsegood, G. N. Parkinson, and A. Fernandez, "A Simple and Sequential Strategy for the Introduction of Complexity and Hierarchy in Hydrogen-Bonded Organic Framework (HOF) Crystals for Environmental Applications," *Angewandte Chemie International Edition* 63 (2024): e202404452, https://doi.org/10.1002/anie.202404452.

159. C. Guo, Y. Gao, S.-Q. Li, et al., "Chemical-Stabilized Aldehyde-Tuned Hydrogen-Bonded Organic Frameworks for Long-Cycle and High-Rate Sodium-Ion Organic Batteries," *Advanced Functional Materials* 34 (2024): 2314851, https://doi.org/10.1002/adfm.202314851.

160. G. Xia, C. Zhou, X. Xiao, Y. Yang, F. Yu, and H. Wang, "Self-Correcting Mismatches in Metastable Hydrogen-Bonded Organic Frameworks With an 11-Fold Interpenetrated Array," *Chemical Science* 15 (2024): 14336–14343, https://doi.org/10.1039/D4SC02751E.

161. L. Chen, H. Yuan, H. Zhao, and B. Li, "Enhancing Ethylene/Acetylene Selective Separation in Hydrogen-Bonded Organic Framework by Modulating Pore Polarity With Bis-Quinoxaline Unit," *Inorganic Chemistry Communications* 174 (2025): 113982, https://doi.org/10.1016/j.inoche.2025.113982.

162. Z.-J. Lin, J.-Y. Qin, X.-P. Zhan, K. Wu, G.-J. Cao, and B. Chen, "Robust Mesoporous Functional Hydrogen-Bonded Organic Framework for Hypochlorite Detection," *ACS Applied Materials & Interfaces* 14 (2022): 21098–21105, https://doi.org/10.1021/acsami.2c05176.

163. J. Liang, S. Xing, P. Brandt, et al., "A Chemically Stable Cucurbit[6]Uril-Based Hydrogen-Bonded Organic Framework for

Potential SO_2/CO_2 Separation," *Journal of Materials Chemistry A* 8 (2020): 19799–19804, https://doi.org/10.1039/D0TA07457H.

164. H. Xiao, H. Ma, M. Han, et al., "A Permanent Porous Hydrogen-Bonded Framework With Room-Temperature Phosphorescence," *Crystal Growth & Design* 21 (2021): 3420–3427, https://doi.org/10.1021/acs.cgd.1c00200.

165. B. Yu, L. Li, S. Liu, et al., "Robust Biological Hydrogen-Bonded Organic Framework With Post-Functionalized Rhenium(I) Sites for Efficient Heterogeneous Visible-Light-Driven CO_2 Reduction," *Angewandte Chemie International Edition* 60 (2021): 8983–8989, https://doi.org/10.1002/anie.202016710.

166. J. Liu, J. Miao, S. Ullah, et al., "A Water-Resistant Hydrogen-Bonded Organic Framework for Ethane/Ethylene Separation in Humid Environments," *ACS Materials Letters* 4 (2022): 1227–1232, https://doi.org/10.1021/acsmaterialslett.2c00370.

167. T. Stolar, J. Alić, I. Lončarić, et al., "Sustainable Solid Form Screening: Mechanochemical Control Over Nucleobase Hydrogen-Bonded Organic Framework Polymorphism," *Crystal Engineering Communications* 24 (2022): 6505–6511, https://doi.org/10.1039/D2CE00668E.

168. J. Chu, Z. Liu, J. Yu, et al., "Boosting H^+ Storage in Aqueous Zinc Ion Batteries via Integrating Redox-Active Sites Into Hydrogen-Bonded Organic Frameworks With Strong π-π Stacking," *Angewandte Chemie International Edition* 63 (2024): e202314411, https://doi.org/10.1002/anie.202314411.

169. Y. Wu, Y. Wang, F. Wei, et al., "Engineering Cyano Groups Into Hydrogen-Bonded Organic Supramolecules With Multi Redox Centers for High-Performance Li-Ion Battery Cathode," *Energy Storage Materials* 63 (2023): 102993, https://doi.org/10.1016/j.ensm.2023.102993.

170. Y. Song, S. Zhu, L. Liu, S. Xiang, Z. Yao, and Z. Zhang, "Increasing Porosity in Hydrogen-Bonded Organic Frameworks for Low-κ Interlayer Dielectric," *Inorganic Chemistry Frontiers* 10 (2023): 4503–4509, https://doi.org/10.1039/D3QI00570D.

171. M. Carrera, I. Such-Basáñez, J. P. Marco-Lozar, et al., "Rational Design of 7-Azaindole-Based Robust Microporous Hydrogen-Bonded Organic Framework for Gas Sorption," *Angewandte Chemie International Edition* 64 (2025): e202412981, https://doi.org/10.1002/anie.202412981.

172. Y. Cai, Y. Zheng, Y. Chen, R. Wei, H. Xu, and J. Gao, "A Solid-State Transformation of Hydrogen-Bonded Organic Frameworks for Efficient Acetylene Storage and Gas Separation," *Chemistry & Biology Engineering* 1 (2024): 615–622, https://doi.org/10.1021/cbe.3c00100.

Supporting Information

Additional supporting information can be found online in the Supporting Information section.

Supporting File 1: anie73521-sup-0001-SuppMat.docx.

Table for detailed information on HOFs with permanent porosity [159–172].

Biographies

Taito Hashimoto received his B.Eng. degree in 2022 and M.Eng. degree in 2024 from Osaka University. He is currently a doctoral student at the Graduate School of Engineering Science, the University of Osaka. His research interests include the design and structural investigation of multicomponent porous crystals and their dynamic behaviors.

Ichiro Hisaki received his Ph.D. degree from Osaka University in 2005 under the supervision of Professor Dr. Yoshito Tobe. After being a JSPS postdoctoral researcher in the group of Professor Dr. Atsuhiro Osuka at Kyoto University, he joined the group of Professor Dr. Mikiji Miyata at Osaka University in 2005 as an assistant professor. In 2018, he moved to the group of Professor Dr. Takayoshi Nakamura at Hokkaido University as an associate professor. Since 2020, he has been a professor at the Graduate School of Engineering Science, the University of Osaka. His current interest is the development of porous functional crystalline materials.